




Chair of Reservoir Engineering

Master's Thesis



Integrated Modeling of Underground  
Hydrogen Storage – Viking A Field, the  
North Sea

Mohab Abdellatif Mohammed Abdellatif

November 2022



**AFFIDAVIT**

I declare on oath that I wrote this thesis independently, did not use other than the specified sources and aids, and did not otherwise use any unauthorized aids.

I declare that I have read, understood, and complied with the guidelines of the senate of the Montanuniversität Leoben for "Good Scientific Practice".

Furthermore, I declare that the electronic and printed version of the submitted thesis are identical, both, formally and with regard to content.

Date 02.11.2022

---

Signature Author  
Mohab Abdellatif Mohammed Abdellatif

Mohab Abdellatif  
Master Thesis 2022  
Petroleum Engineering

# Integrated Modeling of Underground Hydrogen Storage – Viking A Field, the North Sea

Supervisor: Dr. Siroos Azizmohammadi  
Co-supervisor: Dr. Mehrdad Hashemi

Chair of Reservoir Engineering

*To my beloved wife who is always there to stand by me*

## Acknowledgments

Finally, the hard journey came to an end. It wasn't as easy as it may look, but with the help of the people surrounding me, I proudly managed to finish my thesis, and I am utterly grateful to all those who helped me pass this journey successfully. Therefore, I would like to thank all professors and staff at Montanuniversität who were extremely cooperative and helpful in all aspects.

First, I would like to express my sincere gratitude and appreciation to my supervisors, Dr. Siroos Azizmohammadi and Dr. Mehrdad Hashemi, for their endless support and guidance during my thesis. I have learned a lot from them.

I would also like to thank Prof. Holger Ott for ongoing guidance through my master study at Montanuniversität Leoben.

Lastly, I gratefully acknowledge Computer Modeling Group (CMG) for providing the necessary licenses for this study. Special thanks to Faraj Zarei and Reza Malakooti for their generous support during my thesis.

Mohab Abdellatif

Leoben, November 2022



## Abstract

The demand for alternative sustainable energy sources has become higher and more inevitable than ever. Due to the lack of conventional sources, in addition to their environmental and politically related issues, different energy sectors are now focusing on looking into new renewable and reliable sources of energy, such as wind and solar, to meet energy needs. However, the main disadvantage of these sources is the considerable unconformity between production and consumption, which necessitates the reliability of conventional sources or the availability of large energy storage systems. Hydrogen can be utilized as an energy carrier and stored in underground reservoirs to provide the necessary energy storage system required to shrink the seasonal gap between the production and consumption of energy. However, the utilization of hydrogen is accompanied by challenges. Hydrogen is the lightest molecule on earth, hydrogen density is almost eight times less than methane; accordingly, in addition to its higher diffusivity and chemical, and bio-chemical activity, hydrogen behaves differently compared to natural gas. This study presents underground hydrogen storage technology, its state-of-art technologies, and the challenges this technology faces. To sense practically these challenges, a conceptual model is built to investigate the different parameters' effect on the performance of the UHS. The effects of cushion gas type, diffusion, and biochemical activity are analyzed and interpreted. Moreover, the effect of completion configuration and the reservoir dimensions are investigated. Then the application is transferred to a real field study. For this study, the Viking A field in the North Sea was selected as a potential site for underground hydrogen storage. As the North Sea is stacked with tens of wind farms, it would be valuable to have such an energy storage facility in the area. Furthermore, Viking A is a depleted gas reservoir with a recovery factor of more than 90%, thus a lot of information is available about that field, and not much hydrocarbon will be lost. All these reasons make Viking A a good candidate for UHS in the North Sea. A sensitivity analysis study is performed, and different scenarios and strategies are defined to evaluate the impact of different parameters on the performance of UHS in a real field.

# Zusammenfassung

Die Nachfrage nach Quellen nachhaltiger, alternativer Energie ist höher denn je zuvor und hat eine neue Unausweichlichkeit gewonnen. Infolge des Mangels an konventionellen Quellen und deren ökologischen sowie politischen Problematiken, sind verschiedene Energiesektoren mittlerweile darauf fokussiert, nach neuen zuverlässigen Energiequellen wie Wind und Gas zu suchen, um den Energiebedarf zu decken. Jedoch sind diese Energiequellen mit Nachteilen verbunden: Hauptsächlich ist hier die signifikante Nichtkonformität zwischen Produktion und Verbrauch zu nennen, welche die Zuverlässigkeit konventioneller Quellen oder aber die Verfügbarkeit großer Energiespeichersysteme erfordert. Wasserstoff kann als Energieträger genutzt und in unterirdischen Reservoirs gelagert werden — und so das notwendige Energiespeichersystem bieten, um saisonale Lücken zwischen der Produktion und dem Verbrauch von Energie zu verringern. Jedoch bringt die Nutzung von Wasserstoff eigene Herausforderungen mit sich. Wasserstoff ist das leichteste Molekül der Erde. Die Dichte von Wasserstoff ist beinahe achtmal geringer als die von Methan. Wasserstoff verhält sich dementsprechend, zusätzlich zu den Auswirkungen seiner höheren Diffusität und seiner chemischen und biochemischen Aktivität, anders als natürliches Gas. Diese Studie stellt Underground Hydrogen Storage (UHS) vor, präsentiert deren state-of-art Technologien, und diskutiert die Herausforderungen, vor denen diese Technologie steht. Für eine bessere praktische Nachvollziehbarkeit dieser Herausforderungen wird hier ein konzeptionelles Modell gebaut, um die Effekte verschiedener Parameter auf die Leistung von UHS zu untersuchen. Die Effekte von kissenartigen Gastypen, Diffusion, sowie biochemische Aktivität werden analysiert und die daraus resultierenden Daten anschließend ausgewertet. Darüber hinaus untersucht diese Arbeit die Effekte von Fertigstellungskonfigurationen und Reservoirgrößen. Im Anschluss wird dieses Modell auf eine reale Feldstudie übertragen. Für diese Studie wurde das Feld Viking A in der Nordsee als ein potenzieller Standort für Underground Hydrogen Storage ausgewählt. Da in der Nordsee bereits Dutzende Windfarmen angesiedelt sind, wäre die Verfügbarkeit einer solchen Energiespeicheranlage in dieser Region besonders wertvoll. Abschließend wird im Rahmen einer Studie eine Sensibilitätsanalyse durchgeführt. Zudem werden verschiedene Szenarien und dazu passende Strategien ausgearbeitet, um den Einfluss von diversen Parametern auf die Leistung eines UHS in einem realen Feld zu evaluieren.



# Table of Contents

The table of contents below is automatically generated by Word. To update this after revisions, right-click in the table and choose “*Update Field*” for the entire table.

Acknowledgments .....	v
Abstract.....	vii
Zusammenfassung .....	viii
Chapter 1: Introduction.....	11
1.1 Hydrogen Production.....	14
1.2 Hydrogen utilization to store energy.....	15
1.3 Technical statement .....	16
Chapter 2: Literature Review.....	17
2.1 UHS challenges.....	19
2.2 UHS projects and field trials.....	22
Chapter 3: Conceptual Model .....	25
3.1 Model setup.....	25
3.2 Base case.....	26
3.3 Sensitivity Analysis .....	27
Chapter 4: Viking A Field Model .....	35
4.1 Field Description.....	35
4.2 Viking A reservoir geometry .....	37
4.3 I/O Control .....	38
4.4 Reservoir .....	38
4.5 Components .....	39
4.6 Rock-Fluid .....	39
4.7 Initial Conditions .....	40
4.8 Numerical.....	40
4.9 Well and Recurrent .....	40
Chapter 5: Simulation of UHS in Viking A Field.....	43
5.1 Base Case.....	43
5.2 Integrated Asset Model with CoFlow .....	46
Chapter 6: Sensitivity Analysis.....	51
6.1 Cushion gas type .....	51
6.2 Diffusion effect .....	53
6.3 Extended/longer fill-up period.....	54
6.4 Increased injection rate .....	57
6.5 Shifted injection period.....	58
Chapter 7: Conclusion.....	61

7.1	Summary .....	61
7.2	Future Work .....	62
	References .....	63
	List of Figures .....	67
	List of Tables .....	69
	Abbreviations .....	71

# Chapter 1

## Introduction

The impacts of climate change are catastrophic to nature and people, threatening the health of our planet, which eventually will lead to insecure future in all aspects. In the latest report of Intergovernmental Panel on Climate Change (IPCC) (H.-O. Pörtner et al. 2022), they highlighted the impacts of climate change and provided the necessary actions to adapt such phenomenon. Unfortunately, some of these impacts, as stated in their report, are irreversible as they exceeded nature and human systems ability to adapt. Figure 1-1 shows the effected subsystems of ecosystems and human systems due to climate change with the level of confidence based on the evidence available for each system regionally, and it is obvious how widespread are the impacts of climate change. The target is to maintain the global warming below 1.5°C relative to 1850 – 1900 period. Although, this level will still cause unavoidable risks with very high confidence, but it is more adaptable compared to higher warming levels. In this context, 196 countries adopted the Paris Agreement (United Nations Framework Convention on Climate Change 2016), with the goal to limit global warming below 1.5°C. Greenhouse gas emission is a direct contributor to the climate change we are witnessing. Therefore, reducing greenhouse gas emission is a main measure to mitigate the impact of global warming and aids in keeping the 1.5°C limit.

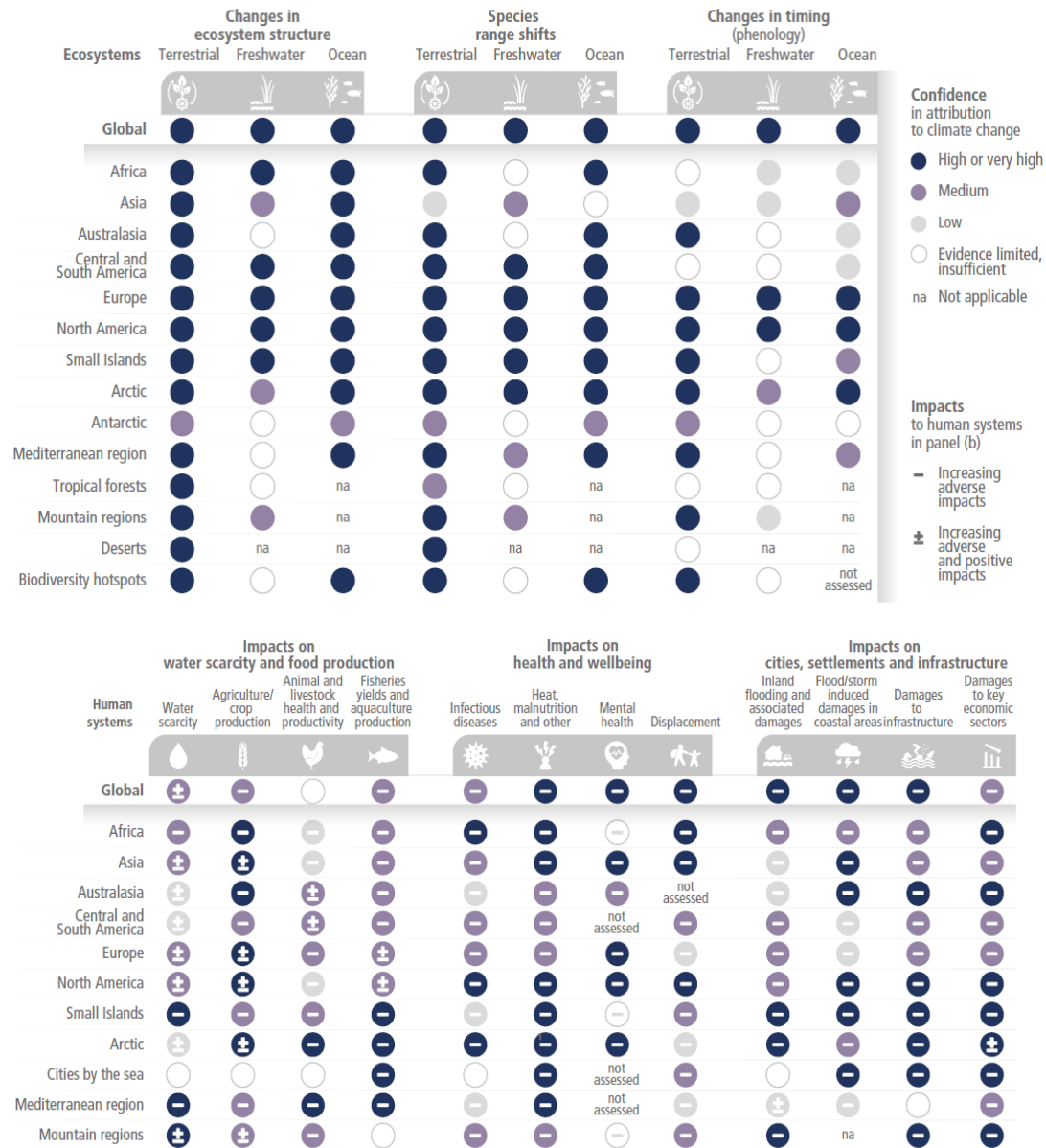


Figure 1-1: Observed global and regional impacts due to climate change on the ecosystems and human systems (H.-O. Pörtner et al. 2022)

Following Paris Agreement and implementing its articles, the world now is gradually transforming from fossil fuels towards carbon-neutral fuels. Several initiatives have been taken in these regards. The Clean Energy for all Europeans (European Commission. Directorate General for Energy. 2019) is one the strong initiative Europe has taken to tackle the energy transition to ensure clean and fair energy transition. They are targeting by 2030 at least 40% cut in greenhouse gas emissions, 32% renewables in energy consumption, and 32.5% energy efficiency, which in turn will lower the EU reliance of imported energy mainly in the form of oil and gas to make the energy supply more secure and fight against any possible blackouts in case of emergencies.

However, fully reliance on renewable energy sources such as wind and solar energy still under research. As such energy sources are highly weather dependents and the electricity produced is highly fluctuating. As we can see from Figure 1-2, during summer Austria has an excess in electricity and lack of electricity during winter.

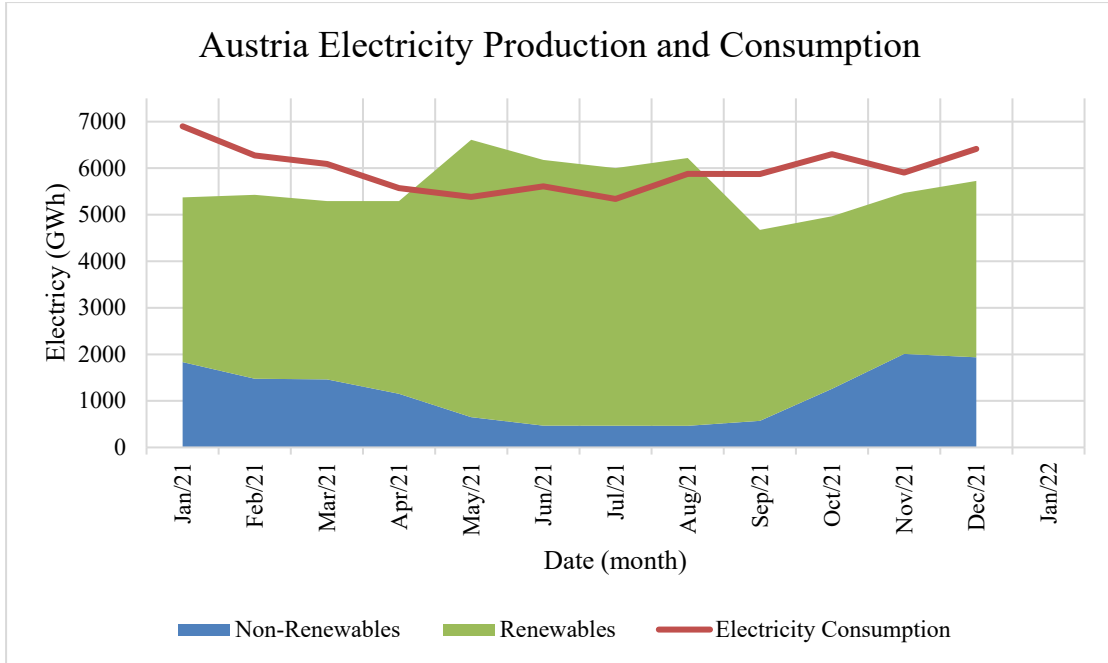


Figure 1-2: Electricity Net Production and Consumption of Austria in 2021 (IEA 2022)

This fluctuating nature of produced electricity, which is not matching with the consumption rates, necessitates the presence of huge energy storage system. Figure 1-3 shows the storage capacity for different energy storage technologies versus the discharge time. We can see that hydrogen can be used effectively as energy carrier to store the electricity with high discharge rate and huge capacity.

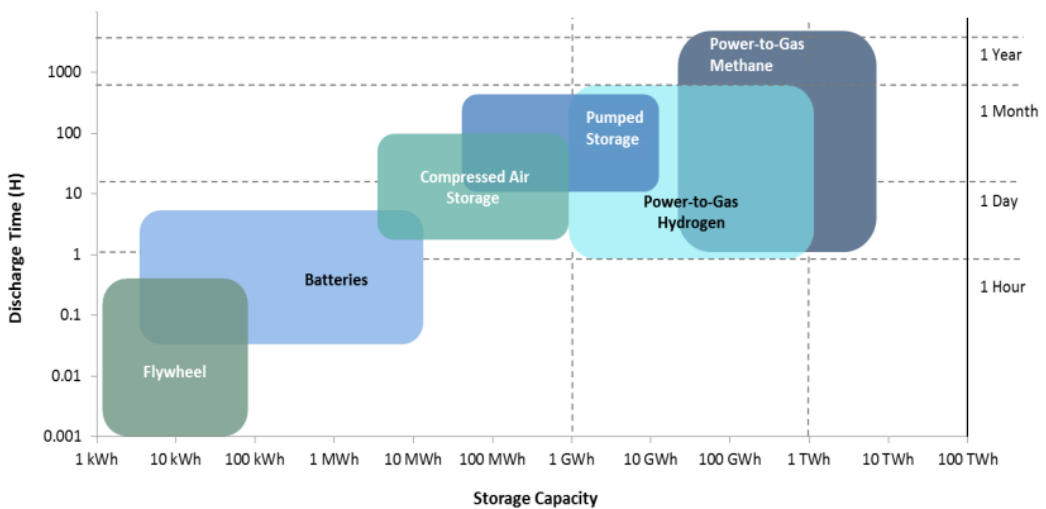


Figure 1-3: Storage capacity for different energy storage technologies (Moore and Shabani 2016)

## 1.1 Hydrogen Production

Hydrogen can be produced through different processes. However, most of these processes are not fully clean as more than 95% of the produced hydrogen comes from fossil fuels (Wang et al. 2021). The hydrogen demand in 2020 was estimated to be 90 Mt which was met entirely from fossil fuels (IEA 2021). As Figure 1-4 shows Natural gas is the main fuel for hydrogen production, mainly using Steam Methane Reformation (SMR) method where the natural gas is heated with steam to produce hydrogen. Also, researchers are developing numerous methods to produce clean low-carbon hydrogen from water splitting with solar energy and from conventional methods they are attempting to provide the heat from the solar energy rather than from burning methane or coal to decrease the greenhouse gas emissions (Wang et al. 2012). There are different methods for producing hydrogen from water splitting technology such as, thermochemical methods where the water molecules are split by thermal energy or in the presence of auxiliary chemicals to enhance the process (BAYKARA 2004), second water splitting method is water electrolysis where the water is split using electric current that passes through two electrodes immersed in water then the hydrogen will be produced on the cathode surface as (Wang et al. 2012) suggests, and to avoid confusion with other methods such as photoelectrolysis, the term “water electrolysis” should only be used when the electricity is provided from an external source that is driven by solar energy. Third water splitting method is Photoelectrolysis and photoelectrochemical, this differs from the previous method only in the way by which the electricity is produced (Licht 2003). Water splitting methods have the lowest water footprint, 9 kg of water per 1 kg of H<sub>2</sub> production (IEA 2021).

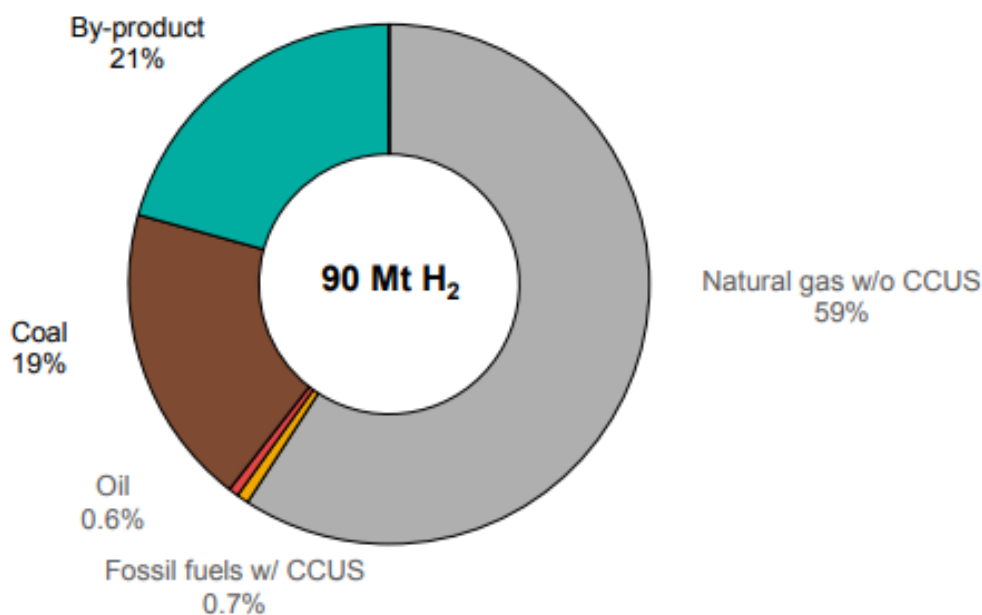


Figure 1-4: Sources of Hydrogen Production (IEA 2021)

Note: CCUS: carbon capture, utilization and storage.

## 1.2 Hydrogen utilization to store energy

Hydrogen has been considered as an attractive energy source and carrier, specially recently and in compliance with the global energy transition strategy to reduce the reliance on fossil fuels such as oil.

Table 1-1 shows a comparison between the characteristic features of hydrogen and methane, we can see that methane is almost eight times denser than hydrogen, thus, to store same mass, hydrogen would require more pressure. Also, we see the low viscosity of hydrogen makes it more mobile than methane, this low viscosity means lower residual hydrogen during withdrawal, but on the other hand while injection due to its higher mobility, hydrogen wouldn't displace efficiently the native fluids in the storage and fingering would occur.

*Table 1-1: Comparison of the characteristic features of hydrogen and methane (Acar and Dincer 2020)*

Characteristic feature	Hydrogen	Methane
Molar mass (kg/kmol)	2.02	16.04
Density (kg/m <sup>3</sup> )	0.09	0.66
Viscosity (Pa.s)	$0.89 \times 10^{-5}$	$1.1 \times 10^{-5}$
Solubility in water (mol/kg <sub>w</sub> )	$7.9 \times 10^{-4}$	$1.4 \times 10^{-3}$
Diffusivity in air (cm <sup>2</sup> /s)	0.61	0.16
Flammability range (vol. %)	4-75	5-15
Auto-ignition Temperature (°C)	585	450
Minimum ignition energy (mJ)	0.02	0.29
Lower heating value (MJ/kg)	120	50
Higher heating value (MJ/kg)	142	56

Hydrogen has higher heating value per unit mass than methane but due to the low density of hydrogen it has lower heating value per unit volume than methane but still has very high energy potential. The energy which is needed to produce hydrogen is higher than the energy that could be produced from hydrogen. However, because of its capabilities that can store huge amount of energy, hydrogen is considered as an efficient energy carrier.

One of the advantages that hydrogen has, is that hydrogen has lower solubility in water, and thus, lower loss in the subsurface storage, but on the other hand, it is highly diffusive compared with methane and thus more susceptible for leakage into cap rock.

In comparison with other large-scale storage options such as pumped hydro schemes and compressed air energy storage system, hydrogen is the only storage option that can store large

volumes of electrical energy, Figure 1-5 shows the preferred storage technology for different operating conditions in terms of period of storage and volume of energy. And from economical point of view, pumped hydro systems and CAES are more economical for smaller volumes of energy when compared with hydrogen, but for larger volumes hydrogen is the better choice (Stolten 2010).

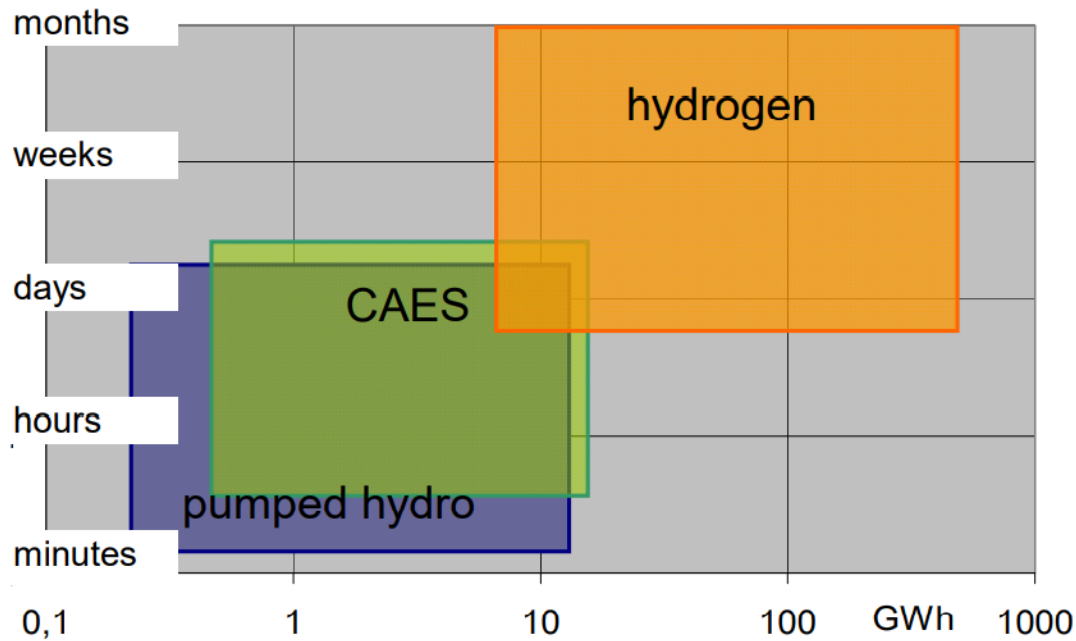


Figure 1-5: Preferential areas of large-scale storage options (Stolten 2010)

### 1.3 Technical statement

Underground hydrogen storage is not on spur of the moment thing, rather it is there since 1970s, and generally the idea of underground gas storage is much older. In this dissertation we will try to state the development of UHS along with examining its challenges:

- Energy capacity
- Hydrogen loss
- Storage integrity
- Hydrogen diffusion
- Biochemical activity

In this course, and to practically test these parameters, we first will build a conceptual model (shoe box model) and investigating the different effects on the storage performance. Then we apply these investigations on a real field in the North Sea as potential for UHS. We selected Viking A field in the southern North Sea for our study and will utilize it as buffer for the huge electricity being produced from the exiting wind farms in addition to the planned ones.



# Chapter 2

## Literature Review

It has been proven that hydrogen can be utilized as an energy carrier to store the surplus energy during low energy consumption and regenerate the energy during high energy consumption.

The concept of underground storage of gases was first introduced in 1915 in a partially depleted gas field of Ontario, Canada (Zivar et al. 2021). And due to this similarity between UHS and natural gas storage, most of the underground hydrogen storage projects make use of the experience gained from natural gas storage but of course with considering the physical and chemical differences between hydrogen and natural gas, as hydrogen is more chemically active and has high affinity for chemical, biological, and microbial reactions underground, in addition to the physical properties of hydrogen such as high diffusivity, low viscosity, and high mobility. All these chemical and physical features of hydrogen make it more complicated with hydrogen storage as hydrogen is more susceptible for leakage and loss and hence energy loss.

Conventionally, hydrogen is stored at surface in small quantities for industrial reasons. The idea of storing hydrogen underground is not new. Since 1956 Baynes gas reservoir had been utilized to store hydrogen (as part of the town gas 50-60% of which is hydrogen) and one of the very early attempts to store hydrogen in the underground was in developed in England by Imperial Chemical Industries to utilize brine-compensated caverns to store hydrogen, and this stored hydrogen is consumed by nearby industrial plants in the production of ammonia and methanol (Foh et al. 1979). At the first world hydrogen energy conference, they carried out a comparison between underground hydrogen storage and natural gas storage, and their main conclusion was “no insurmountable or environmental problems” in using underground storages for hydrogen (Veziroğlu 1976). In the investigations that (Carden and Paterson 1979) did on the losses associated with underground hydrogen storage, they identified the losses as “once-only losses” and operating losses. “once-only losses” are attributed to cushion gas cost, trapped gas into the dead-end pores, saturating the connate water which could be up to 0.4% of the first cycle, and

gas leakages. The operating losses, according to their findings, are attributed to mechanical pumping, friction within the borehole, and borehole pressure drop which could be equal to 1% per hydrogen injection cycle. (Taylor et al. 1986) made a detailed comparison between different modes of hydrogen storage (rock caverns, salt caverns, and depleted reservoirs) and economic assessment of each mode, showing that hydrogen storage in salt caverns had the most economic value, similarly (Schaber et al. 2004) compared between different surface storage technologies and underground hydrogen storage. By time, hydrogen storage technology gets more and more attention, and more in-deep studies about the feasibility of UHS are carried out. (Pfeiffer and Bauer 2015) investigated a hypothetical site based on actual geologic data in Schleswig-Holstein, Germany. The aim was to create a storage site to mitigate the energy production gap for one week by optimizing the injection scheme, shut-in periods, and initial filling of the reservoir. (Amid et al. 2016) worked on Rough Gas Facility to compare its energy output against a case where Hydrogen is used as the working gas in that depleted gas reservoir. Phreeqc tool was used to examine the chemical stability of Hydrogen in the reservoir. Several assemblages of minerals in the presence of Hydrogen and water were investigated. And their study resulted in the following, Clay-bearing sandstone and iron oxides were found to be stable under the reservoir condition but the assemblages containing Sulfur were not and H<sub>2</sub>S were produced. Accordingly, much care should be given to choose the right reservoir that either has little Sulphur or too hot to prevent the activity. (Tarkowski and Czapowski 2018) analyzed seven salt domes as promising sites for hydrogen storage, showing the geological conditions favorable for hydrogen storage, and also discussed the advantages of hydrogen storage in depleted reservoirs. (Heinemann et al. 2018) investigated three conceptual hydrogen storage plays in Midland Valley of Scotland and assessed their conditions as future potential targets for pilot projects. (Hassannayebi et al. 2019) studied the geochemical interaction of hydrogen in a depleted gas reservoir in the Molasse Basin in Upper Austria. They proposed a geochemical modeling workflow that results in extensive insight into the contributing mechanisms and risk evaluation in such projects. Their findings show considerable uncertainty in the process due to a lack of experimental and field data. Therefore, the disturbance of reservoir integrity associated with geochemical interactions with hydrogen cannot generally be ruled out, and it is more site-specific that needs particular considerations. (Lemieux et al. 2019) presented an assessment for potential hydrogen storage in geological formations such as salt, rock caverns, depleted oil and gas fields, and aquifers. (Shi et al. 2020) studied the impact of storing a mixture of hydrogen and natural gas in an existing natural gas storage field in California and investigated the reservoir relevant properties on formation samples in terms of permeability, porosity, surface area, mineralogy, and structural characteristics before and after injecting the mixture. Their results show a decrease in caprock permeability after the exposure to the gas mixture which

indicates an improvement of the sealing capacity. . (Wang et al. 2021) performed a 2D simulation with very fine cell size to examine the flow behavior of H<sub>2</sub> with CO<sub>2</sub> as cushion gas. They analyzed the viscous instability, capillary bypassing, gas trapping, and gravity effects. To correlate different scales, they applied three dimensionless groups, including aspect ratio, capillary/viscous ratio, and gravity/viscous ratio. (Okoroafor et al. 2022) investigated the reservoir, geological, and operational controls that affect large-scale hydrogen storage using the ECLIPSE E300 reservoir simulator. They introduced a screening criterion for potential underground hydrogen storage sites and a methodology to rank geological and reservoir properties.

## 2.1 UHS challenges

The existing gas storages can be utilized in the process of hydrogen storage but with limits and challenges due to the different behavior and features of hydrogen compared to natural gas. Both density and viscosity of hydrogen is much lower than that of natural gas which influences the behavior of hydrogen in the porous media.

### 2.1.1 Energy capacity

One of the challenges accompanied with UHS is the volumetric capacity of energy that can be stored. From Figure 2-1 we can see that hydrogen has the highest calorific value per unit mass but the lowest per unit volume compared to other fuels this is because the low density of hydrogen that is almost eight times smaller than that of methane, accordingly, hydrogen is not the best option as a source of energy rather an energy carrier.

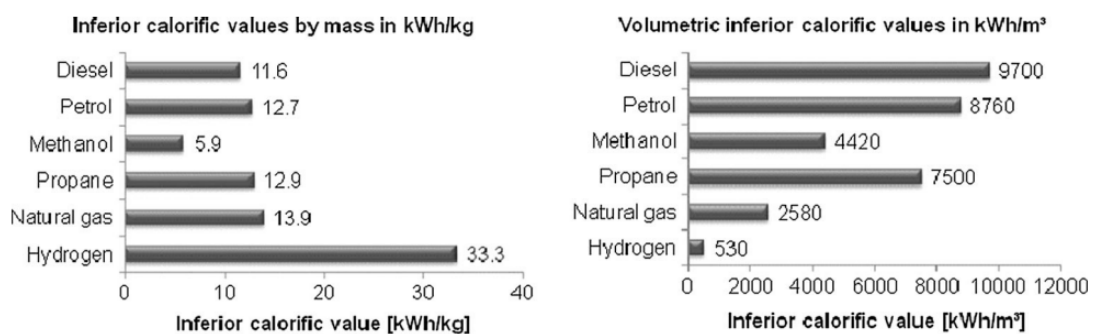


Figure 2-1: Mass and volume calorific values for different fuels at 200 bar and 25 °C (Crotagino F and Hamelmann R 2007)

### 2.1.2 Integrity of the storage

The integrity of the storage is one the main concerns about storage of hydrogen underground. In depleted gas reservoirs, the cap rock and the sealing surroundings have preserved the natural gas for millions of years and in turn expected to act similarly in case we need to store methane

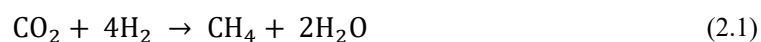
in the reservoir. But this shouldn't be the case when storing hydrogen due to the dissimilarity between hydrogen and methane as explained before. The high capillary threshold of the existing sealing is the mean mechanism to prevent the gas beneath it from further migration, and in case this pressure threshold is exceeded the sealing rock become permeable for the gas and is not sealing anymore.

### **2.1.3 Gas Diffusion**

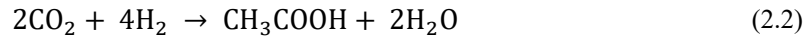
One of the main challenges that UHS face is the mixing of hydrogen with either the native fluids in the storage or the injected cushion gas if not hydrogen, as this will highly affect the purity of the re-produced hydrogen. Therefore, hydrogen diffusivity effect should be included in the feasibility study of UHS, as diffusion is one of the main driving forces that cause mass transfer between hydrogen and other gases. This mass transfer consists of two components: the molecular diffusion and the mechanical dispersion. Molecular diffusion is generally a slow process, but in case of hydrogen storage still need to be considered as the diffusion coefficient of hydrogen is approximately four times that of methane, and it occurs due to the random Brownian motion of the molecules. It is independent of the advective or convective transport thus is the dominating process during the idle periods (Tek 2013). On the other hand, mechanical dispersion is gas mixing process that takes place due to the movement of the gases and the flow velocity profile through pores, low velocity close to the walls of the pores and high velocity in the middle of the pores. This mechanical dispersion is highly dependent on the porous medium tortuosity and heterogeneity. Similarly, hydrogen diffusion into the water saturated caprock and the underlying formations as well should be verified as part of any study for UHS.

### **2.1.4 Microbial activities**

Hydrogen is an electron donor, therefore, it is considered as food for microorganisms. By this microbial activity, hydrogen could be consumed by the microorganisms exist in the reservoir. Several processes could cause this microbial consumption of hydrogen such as (1) methanogenesis, (2) acetogenesis, and (3) sulfate reduction. The methanogenesis occurs in the presence of archaea microorganisms and CO<sub>2</sub> with optimum conditions (Panfilov 2016). The methanogenesis reaction:



In the acetogenesis process, the acetate can be converted to acetic acid based on the following reaction (Panfilov 2016):



In sulfate reduction process, the sulfate reducing bacteria (SRB) consume hydrogen and produce hydrogen sulfide by the following reaction (Baumgartner et al. 2006):



### **2.1.5 Solution in connate water**

The irreducible water in the storage will be exposed to the injected hydrogen, and hydrogen will dissolve in it until the water is saturated and no more dissolution occurs. Therefore, the loss of hydrogen due to solution in connate water is considered as one-time loss or capital loss at the beginning of the project. Though, the solubility of hydrogen in water is very low, it has been proven that the solubility of hydrogen in water depends on the amount and type of ions dissolved in water, as reported in the field study in Austria H2STORE Project (Pudlo et al. 2013) when they used 10% hydrogen in the injected gas, the loss due to solution where estimated to be 0.88%.

### **2.1.6 Viscous fingering**

Hydrogen is the lightest molecule on earth, and thus it is extremely mobile compared to other gases. Viscous fingering occurs in case of fluids displacement, when the displacing fluid is more mobile than the displaced fluid, it intrudes into it and viscous fingering noticed. Therefore, if the mobility ratio is less than one, then a stable displacement will be established, but if the mobility ratio is higher than one, viscous fingering is expected to happen.

### **2.1.7 Gravity override**

Due to low density of hydrogen, gravity is the main driving force in distributing the different fluids in UHS. Hydrogen, with its low density, will migrate upwards and accumulate above other existing fluids. Accordingly, studying the gravity effect in the preparation stage of UHS is extremely important, as it could affect the performance of the UHS. When the hydrogen accumulates in top of the reservoir, the bottom of the well will be exposed to the other gases and this will affect the purity of the re-produced hydrogen, and on the other side, the gravity override can be beneficial to the performance as we can utilize the effect and inject cushion gases, e.g., N<sub>2</sub> to separate between the hydrogen on top of it and the underlying native fluids.

### **2.1.8 Cushion gas**

As an important part of the storage system, UHS requires the so-called cushion gas such as nitrogen, carbon dioxide, methane, and others. The cushion gas mainly plays two roles: pressurizing the reservoir to maintain a required production rate, and act as a barrier between

the hydrogen and the native fluids existing in the storage (Kanaani et al. 2022). Therefore, much care must be given to the selection of the cushion gas in terms of type, volume, injection rate, and its composition, as its compatibility with the existing fluids is vital to avoid further reactions, also part this cushion gas is expected to be produced along with hydrogen, so the separation process should be also considered.

## **2.2 UHS projects and field trials**

Several projects have been launched to investigate the applicability of underground hydrogen storage technology.

### **2.2.1 HyStock Pilot Project**

(HyStock 2019)

The aim of this project is to convert 1 Megawatts of sustainable electricity into green hydrogen, and to store the produced hydrogen in the salt caverns in EnergyStock location at Zuidwending. According to their plan, by the end of 2026 they should have connected the facility to the hydrogen network and fill up the first salt cavern with hydrogen as cushion gas, the capacity of this cavern is estimated to be 200 GWh (= 6,000 tonnes H<sub>2</sub>). By 2030 four caverns should be operational to cover the market demands.

### **2.2.2 The Underground Sun Storage Project**

(RAG Austria AG et al. 2017)

This project was launched in mid-2013 and completed in mid-2017. The target of this project was to investigate possible facilities to store the excess renewable energy in the form of hydrogen. In the first part of the project, they studied the integrity of the storage facility and the feasibility of a field test from geochemical, geophysical, microbiological, and materials point of view to capture the influences that hydrogen injection will have on the integrity of the cap rock, changes in the reservoir behavior, in addition to the hydrogen diffusion and its movement in the reservoir and its reactivity. In the second part of the project and based on the laboratory tests results from the first part, they carried out the field test at a depleted natural gas reservoir in the molasse basin.

For the field test they have chosen Lehen-002 in Vöcklabruck city in the district of Upper Austria. They carried out a complete storage cycle which consists of:

- Injection of hydrogen admixture (NG with almost 10% hydrogen) for about 3 months
- Shut-in for about 4 months
- Gas withdrawal for about 3 months

The results of this field test proved the integrity of the storage from different aspects.

### **2.2.3 Hychico in Argentina**

(A., Pérez: E., Pérez: S., Dupraz: J., Bolcich: 2016)

In 2010 Hychico started their studies for a potential UHS in a depleted gas reservoir near to its hydrogen facilities. The aim of the project is to test the reservoir capacity and its hydrogen tightness. Their results show that hydrogen storage can involve issues such as chemical and bacteriological issues, in addition to changes in reservoir characteristics such as permeability due to interaction with hydrogen. The main constraint was the hydrogen embrittlement that requires selection of proper materials and control of pressure and temperature. Additionally, they launched another pilot project to produce methane from underground biological processes.





# Chapter 3

## Conceptual Model

To sense the challenges that would affect the underground hydrogen storage performance, conceptual “shoe box” model is built to examine the behavior of the UHS under different conditions and the effect of different parameters on a small scale.

### 3.1 Model setup

Figure 3-1 shows a 3D view of the shoe-box model that built using CMG Builder.

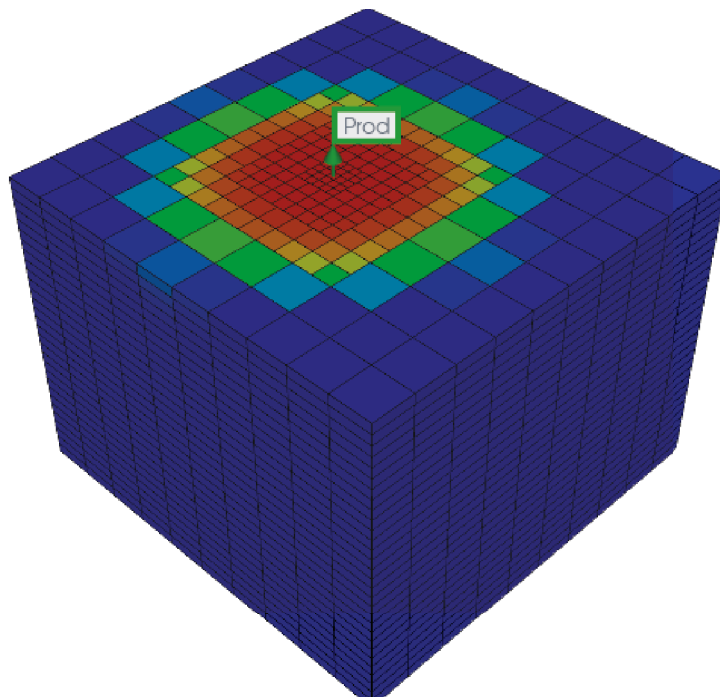


*Figure 3-1: 3D view of the conceptual model*

The model dimensions are  $300 \times 300 \times 30$  FT in X, Y, and Z direction respectively at depth of 3000 to 3030 Ft. The number of parent cells is 10 in X and Y direction and 30 in the Z direction.

The permeability is set to 10 mD in X and Y direction and 5 mD in Z direction. The Porosity is equal to 0.2. We refined the cells around the wellbore to capture the flow behavior in the vicinity of the wellbore. For the rock-fluid model the built-in correlations for well sorted consolidated sandstone is utilized to generate the liquid-gas table. The initial pressure is set to be 400 psi, the water saturation is 0.2 and gas composition is 100% methane.

### 3.2 Base case

In this case, hydrogen is injected into the reservoir during summertime from March to September, then shut-in the reservoir for three months and then reproducing the hydrogen during winter from December to February. The first year is left for preparation of the reservoir such as filling-up period or injecting cushion gas as shown in Figure 3-2.

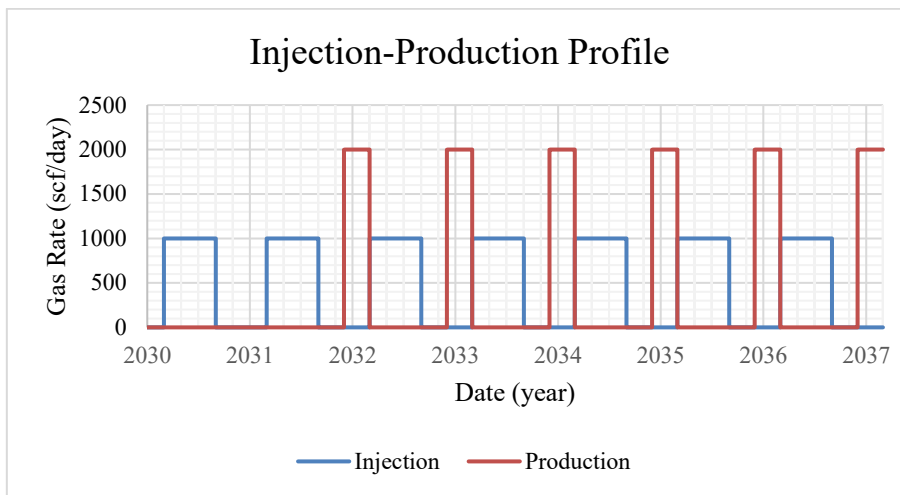


Figure 3-2: Production-Injection profile for the base case of the conceptual model

Table 3-1 shows the strategy followed for the injection and production of the conceptual model.

	Rate	Period
Fill-up	1000 scf/day	6 months (March-September)
Shut-in	--	3 months (September-November)
Production	2000 scf/day	3 months (December-March)
Injection	1000 scf/day	6 months (March-September)

Table 3-1: Base case strategy for the conceptual model

	Rate	Period
Fill-up	1000 scf/day	6 months (March-September)
Shut-in	--	3 months (September-November)
Production	2000 scf/day	3 months (December-March)
Injection	1000 scf/day	6 months (March-September)

As shown in Figure 3-3 the pressure builds up during injection of hydrogen. Though we are producing exactly what we inject in volume, after each production cycle the pressure is not restored to the preceding level, and we see continuous increase in the pressure. This is attributed to the fact that; hydrogen has higher compressibility factor than methane, and after each cycle the volume of hydrogen in the reservoir is increased, because pure hydrogen is injected, but a mixture of hydrogen and methane is produced as shown in Figure 3-4, and at the end of each cycle almost 50% methane and 50% hydrogen are produced.

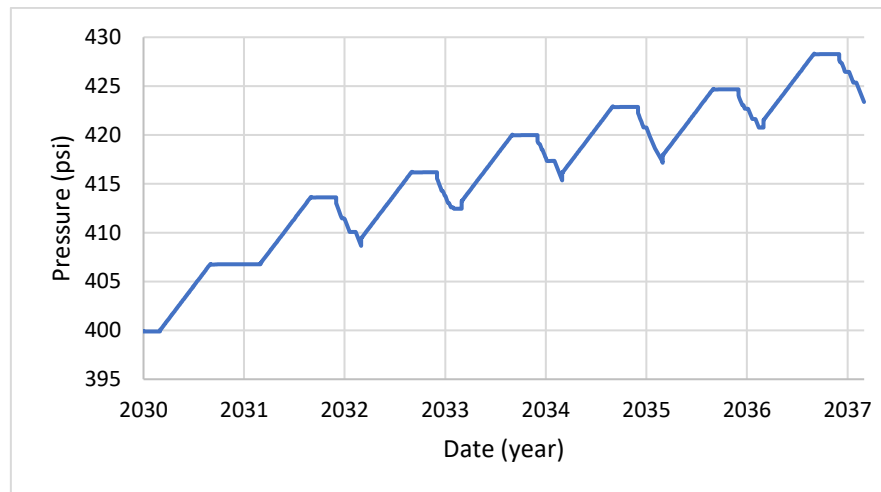


Figure 3-3: BHP during injection and production

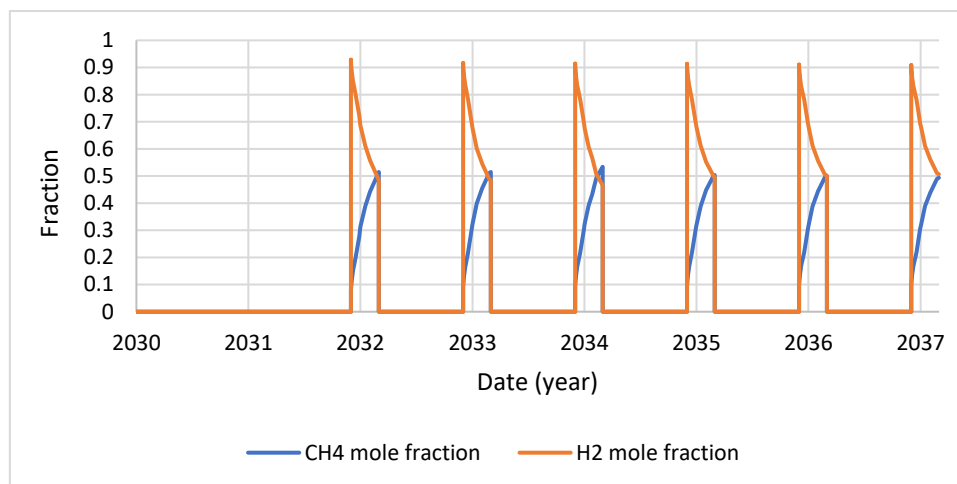


Figure 3-4: Mole fraction of the produced gas

### 3.3 Sensitivity Analysis

#### 3.3.1 Different cushion gases

The role of the cushion gas in UHS is to act as a barrier between the hydrogen and the native fluids in addition to pressurizing the reservoir for better performance. Therefore, instead of

filling-up the reservoir with hydrogen in the first year, and lose this volume of hydrogen into the reservoir, several types of cushion gases; methane, nitrogen, carbon dioxide, and helium are examined.

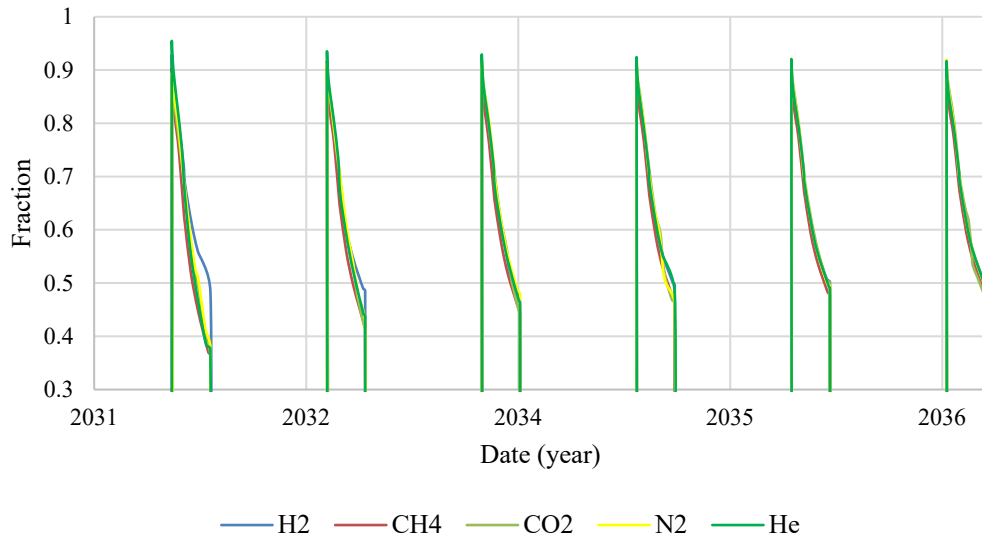


Figure 3-5: Hydrogen mole fraction in the produced gas

As can be seen in Figure 3-5 that different types of cushion gases act very similar to hydrogen as filling up gas especially at later cycles.

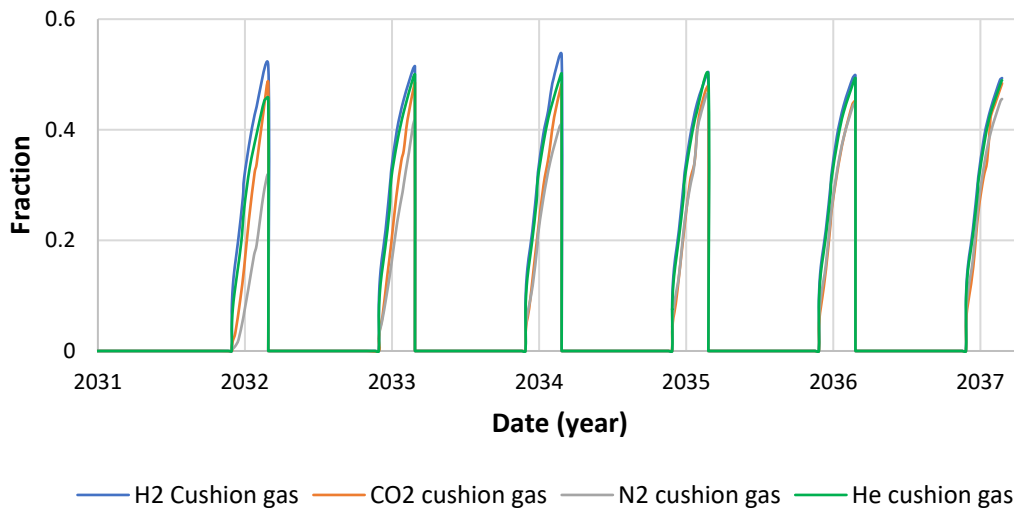


Figure 3-6: Mole fraction of methane in the produced gas

Figure 3-6 shows the mole fraction of methane when using different types of cushion gases, it is noticed that at the first cycle nitrogen acts as the most efficient barrier to the native fluids in the reservoir. This is attributed to the density difference with the native fluids, the reservoir is initially filled with methane, thus too light gases like helium and hydrogen accumulated at the top of the reservoir and therefore the bottom of the well is exposed to the native fluids.

Similarly, carbon dioxide is much heavier than the methane, thus accumulated at the bottom of the well and the top part is exposed to the native fluids as shown in Figure 3-7. And from this it is concluded that the best cushion gas type that act as a barrier is the one with density as close as possible to the native fluids.

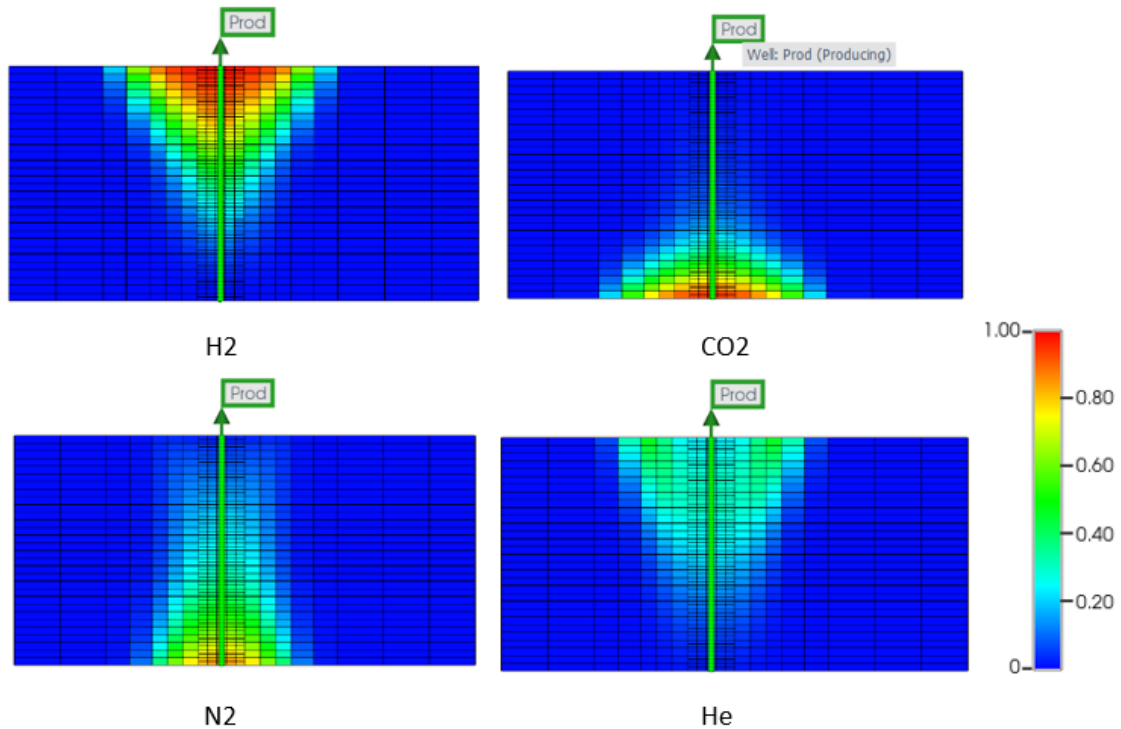


Figure 3-7: Different cushion gases mole fraction at the end of the first cycle

### 3.3.2 Diffusion effect

Hydrogen is a very small and light molecule, the diffusivity of hydrogen in air is almost four times the diffusivity of methane. Thus, diffusivity of hydrogen should be included in a feasibility study of UHS. Therefore, to investigate the effect of gas diffusion, the Sigmund correlation (Sigmund 1976) is defined in the GEM model. Sigmund Diffusivity can be added to our model with the following KEYWORD:

**\*DIFCOR-GAS \*SIGMUND**

The effect of gas diffusivity is not only sensed as hydrogen loss into cap rock due to dispersion into water, but also in the purity of the reproduced hydrogen as hydrogen will diffuse and mix with the other existing gases. Figure 3-8 shows the mole fraction of hydrogen in the produced gas with and without gas diffusion. We can see how dramatically the purity of the reproduced hydrogen decreased due to gas diffusivity. Also, Figure 3-9 shows the distribution of hydrogen in the reservoir after the end of first cycle with and without diffusion. It is seen how the hydrogen diffuses into the reservoir and doesn't accumulate in the vicinity of the well which is considered as a very big loss of hydrogen and affect the performance of the UHS. Accordingly,

considering gas diffusivity and hydrogen diffusivity should be considered in any feasibility study for underground hydrogen storage.

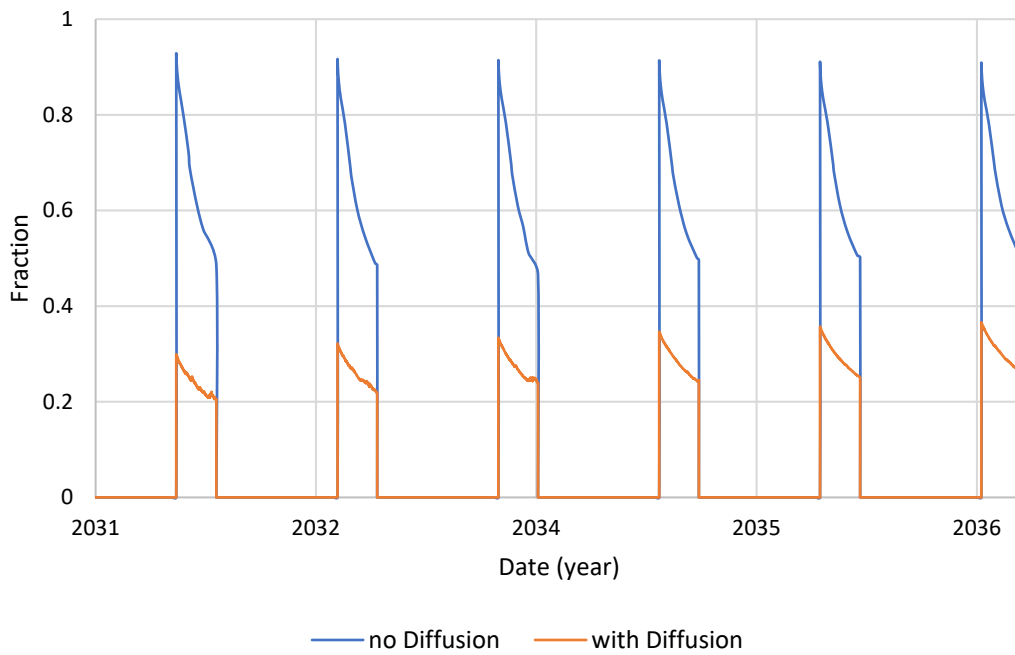


Figure 3-8: hydrogen mole fraction in the produced stream

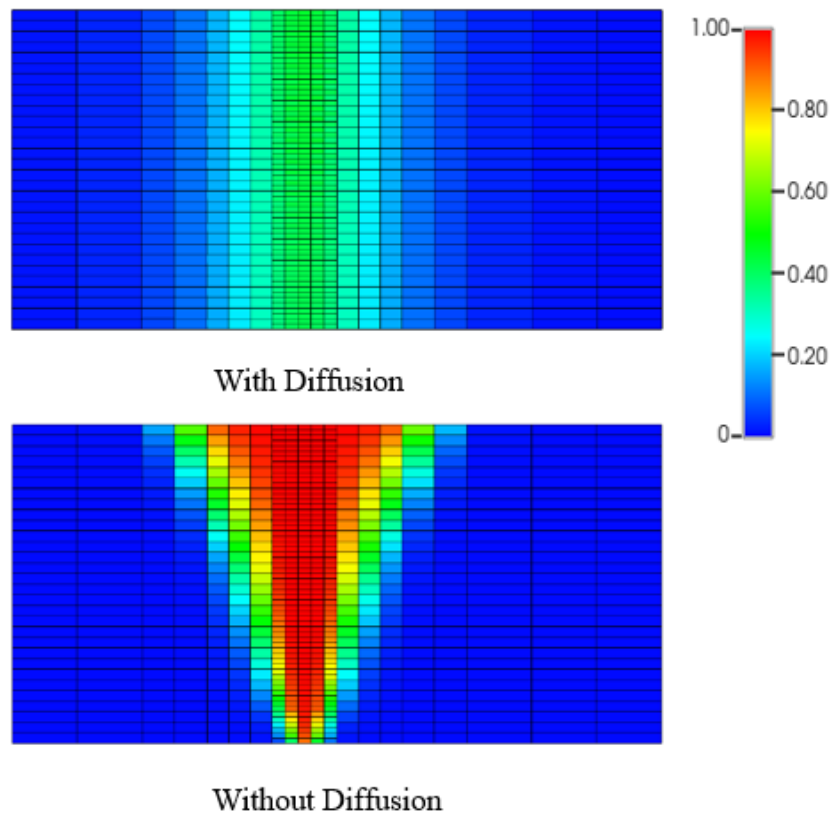


Figure 3-9: Hydrogen mole fraction in the reservoir with and without diffusion after the end of first injection cycle

### 3.3.3 Methanogenesis

During UHS the hydrogen is susceptible to consumption and loss by the biochemical activity. There are several types of biochemical activity that could occur, in this conceptual model the methanogenesis process is simulated. Methanogenesis process occurs due to the reaction of hydrogen and carbon dioxide accelerated by of microorganisms as the following reaction:



Therefore, methanogenesis will be a big concern in case carbon dioxide is used as a cushion gas, or the reservoir already contains carbon dioxide either as free gas or as one of the minerals of the rock. In order to simulate the methanogenesis process in the conceptual model, the reservoir is initialized with 90% methane and 10% CO<sub>2</sub>, other features and strategy is left similar to the case where CO<sub>2</sub> is used as cushion gas in 3.3.

Methanation is activated through the following keywords at the end of the component section of the GEM script:

```
*GEOCHEM_V2
*REACTION-RATE-ARN      'CO2' + 4 'H2' = 'CH4' + 2 'H2O'
*REACTION-ORDER        'CO2' 1 'H2' 1
*FREQUENCY-FACTOR      1.0e-3
*ACTIVATION-ENERGY     0
```

Arrhenius type reaction is used, and reactants order is set to 1. For simplicity activation energy is set to zero and frequency factor is assumed to be 10<sup>-3</sup>.

Figure 3-10 shows the purity of the produced hydrogen. It is obvious how much the purity of the produced hydrogen is reduced due to the consumption of hydrogen due to Methanogenesis process, which in turn will have an effect as well on the BHP as seen in Figure 3-11.

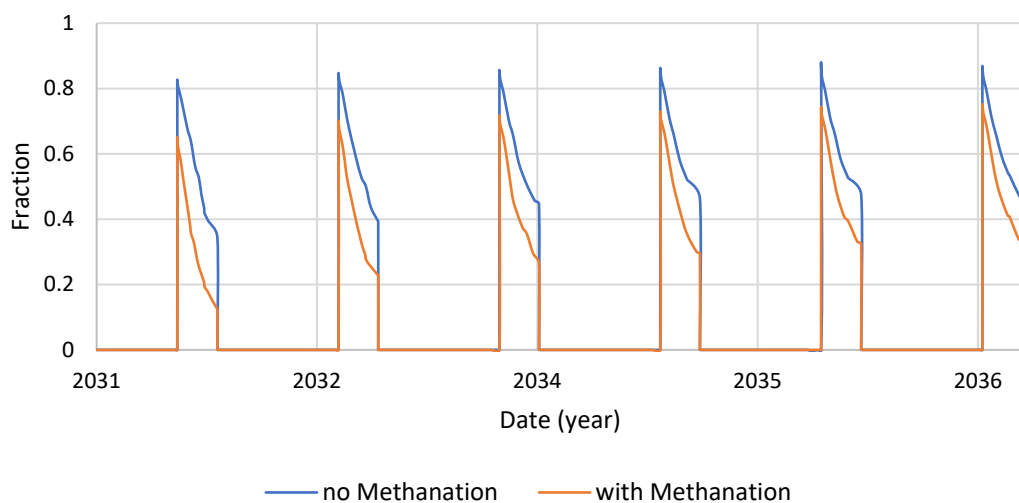


Figure 3-10: Mole fraction of hydrogen with and without methanation

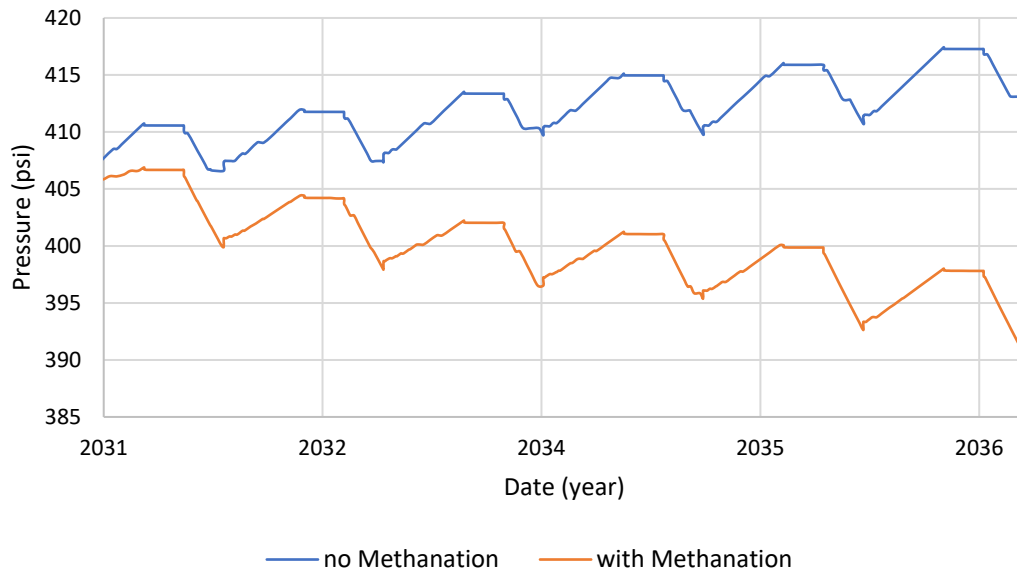


Figure 3-11: Bottom hole pressure with and without methanation

### 3.3.4 Partial perforation

Another factor that should be considered is the configuration of the completion interval. Using the base case 3.2 but this time only the top third of the well is open and the bottom part is plugged during injection and production. Due to the low gravity of hydrogen compared to methane, it accumulates in the top part of the reservoir, therefore the performance of the storage will be enhanced. This can be seen in Figure 3-12, when partially perforate the well and only operate the top third of the well, the purity of the hydrogen increased in the produced gas.

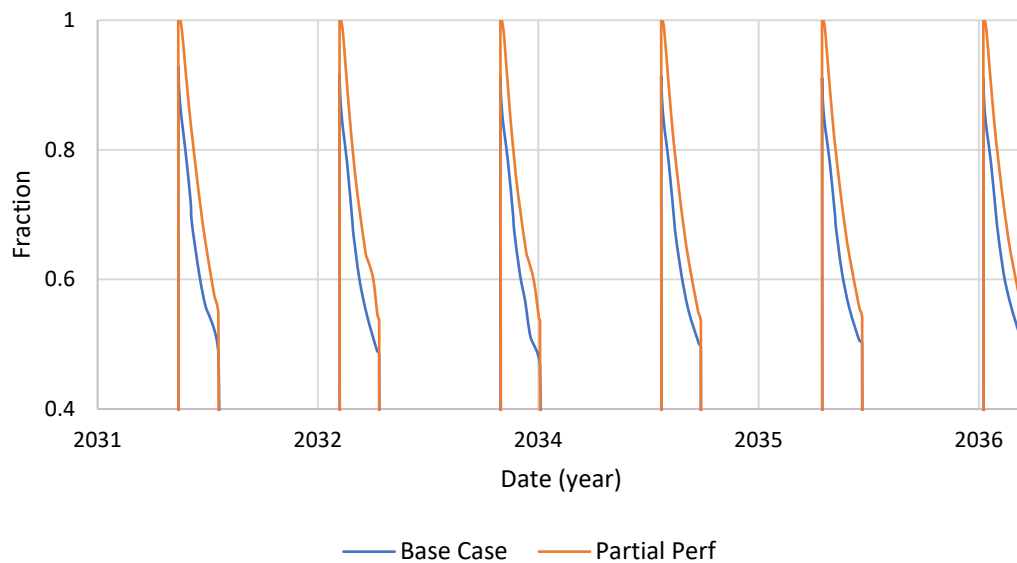


Figure 3-12: Hydrogen mole fraction when isolate the bottom part and only open the top third of the well



### 3.3.5 Reservoir thickness

In this case the thickness of the reservoir is reduced by a factor of 10, that is, reservoir thickness is decreased to 3 ft instead of 30 ft.

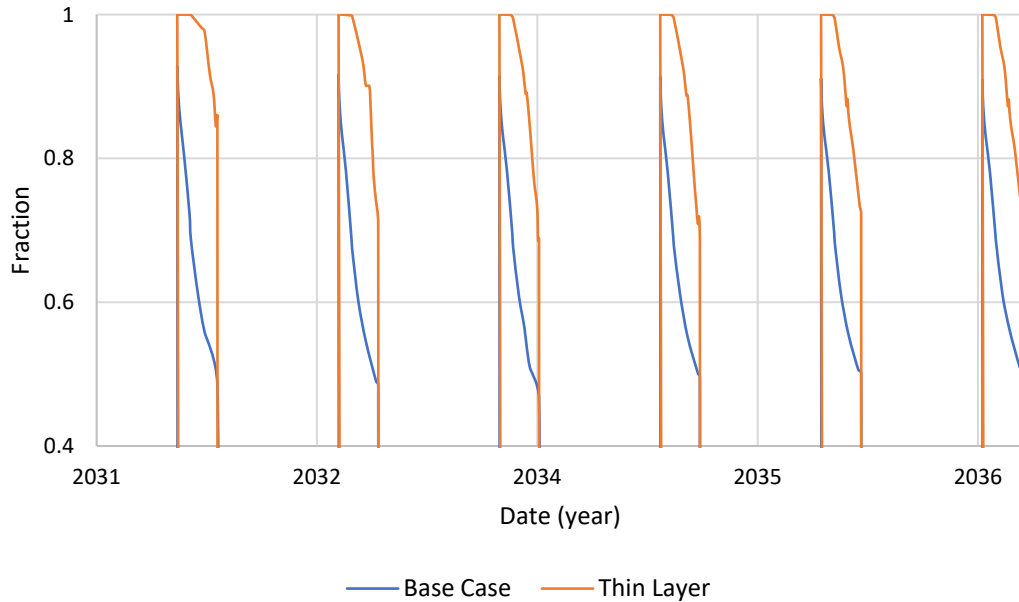


Figure 3-13: Mole fraction of hydrogen in case of thin reservoir against base case

As shown in Figure 3-13, the purity of the produced hydrogen is much increased compared to thicker reservoir in the base case. This is attributed to the fact that, in case of thin reservoir, the gravity override effect was not encountered as the hydrogen is occupying the area around the well, and the well not exposed much to the native fluids in the reservoir.



# Chapter 4

## Viking A Field Model

In the previous chapter, we investigated the different behaviors of hydrogen when stored underground in a conceptual box model. In this chapter we will apply the investigations we did on a conceptual model into a real-field model. For this purpose, we have chosen Viking A as a potential for underground hydrogen storage in the North Sea, for the following reasons: (1) Need for electricity: Electrolysis is green carbon-free hydrogen production from renewable resources. There are tens of wind farms currently operating in the North Sea, at the moment of writing this thesis, Germany, Belgium, the Netherlands and Denmark pledged to build 150 gigawatts of offshore wind capacity in the North Sea to help achieve the EU's climate goals and, eventually, break away from imported energy (AP 2022). Therefore, it would be helpful to have such an energy buffer or temporary storage in the area to store the excess energy generated from these windfarms; (2) the availability of data: Viking A is one of the potential sites selected for Carbon Capture and Sequestration (CCS) projects in the UK offshore. There are several publications on this field and the reservoir model is available for the CCS project (Pale Blue Dot Energy 2017); (3) Almost fully depleted reservoir: It is a highly depleted reservoir with more than 90% recovery ceased in 1991. Thus, not much hydrocarbon will be lost.

### 4.1 Field Description

(Palmer et al. 1995) and (Riches 2003) summarized the development of Viking field and its Description. Figure 4-1 shows the location map of Viking Field in the North Sea. It is located in the Southern North Sea, approximately 140 km east of Lincolnshire, in blocks 49/12a, 49/16, and 49/17. The original field contains nine reservoirs (A, B, C, D, E, F, G, Gn, and H), the whole field together contains approximately 3835 BCF gas-in-place of which 2930 BCF has

been produced with nearly 77% recovery factor as of December 1999. Detailed description of the structure and stratigraphy can be found in (van Hoorn 1987), (ARTHUR 1993), (Stefano Patruno and William Reid 2016), (Ziegler 1977), and (Robert J. Hooper and Colin More 1995).

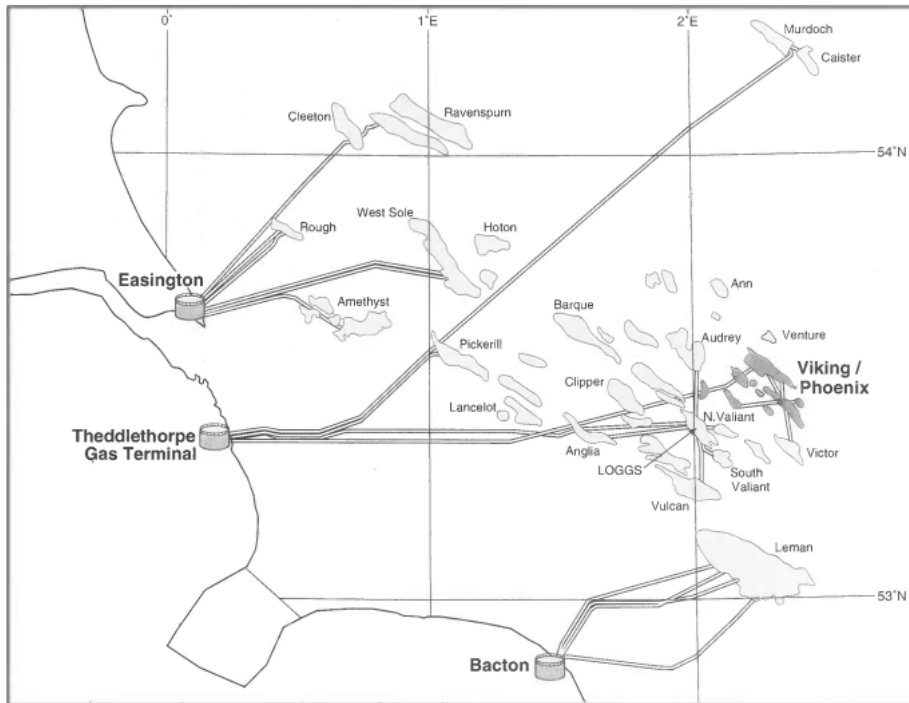


Figure 4-1: Viking Field location map (Riches 2003)

Viking A was discovered by well 49/12-2 in March 1969 and was put into production in October 1972 and was ceased 1991 after production of 1035.42 BCF (NSTA Authority 2022).

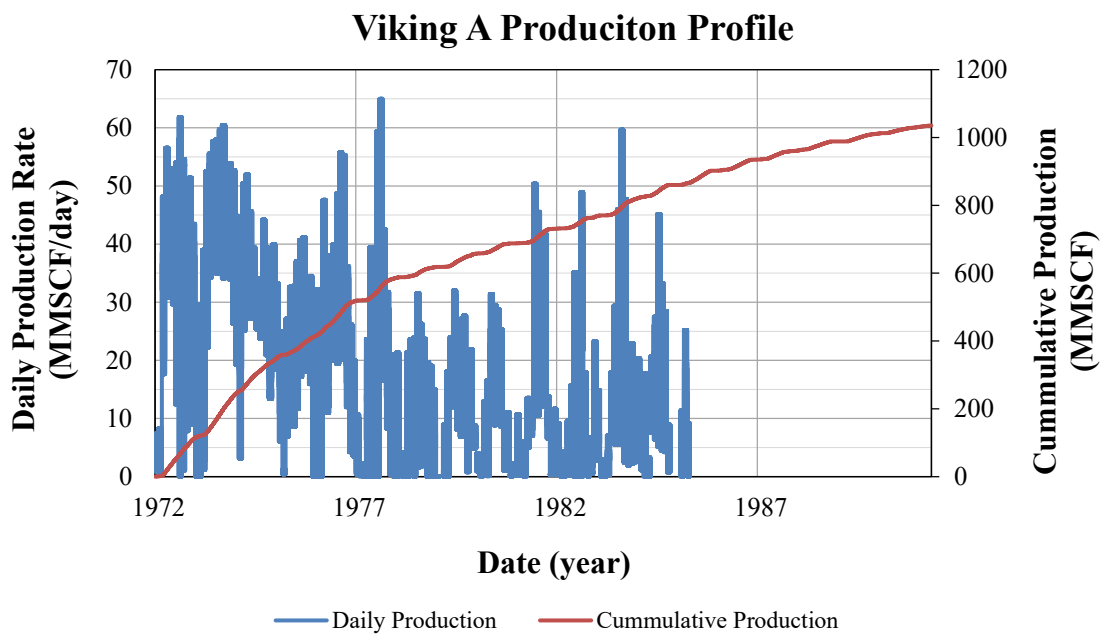


Figure 4-2: Production Profile of Viking A field (NSTA Authority 2022)

Figure 4-2 shows the production profile of Viking A field from start of production in 1972 till 1991. Table 4-1 shows a summary of the properties of the total Viking gas field.

Table 4-1: Viking gas fields data summary (Riches 2003)

<b>Trap</b>	
Type	Tilted/inverted fault blocks
HC contact	Variable 9000-10,200 ft
Gas Column	700 ft max. in the Rotliegendes
Formation	Leman Sandstone Formation
Age	Permian
<b>Reservoir</b>	
Gross thickness	400-700 ft
Porosity	7-25%
Permeability	0.1-100 mD
Water saturation	0.1 average value
Rock Compressibility	$9.814 \times 10^{-7}$ psi <sup>-1</sup>
Reservoir temperature	183 °F average value
Initial pressure	4150-4670 psi
Current pressure	500 psi average value

## 4.2 Viking A reservoir geometry

The Department for Business, Energy, and Industrial Strategy is appraising several potential sites for carbon capture and sequestration projects offshore in the UK. Viking A is one of these potential sites for CCS (Pale Blue Dot Energy 2017). For our study, we utilized the Eclipse model they built for their project and extracted RESCUE files to import it in CMG. The reason why we selected CMG for our simulation, is that GEM simulator can simulate hydrogen component and integrate the model in CoFlow also. Figure 4-3 shows the 3D grid of Viking A reservoir.

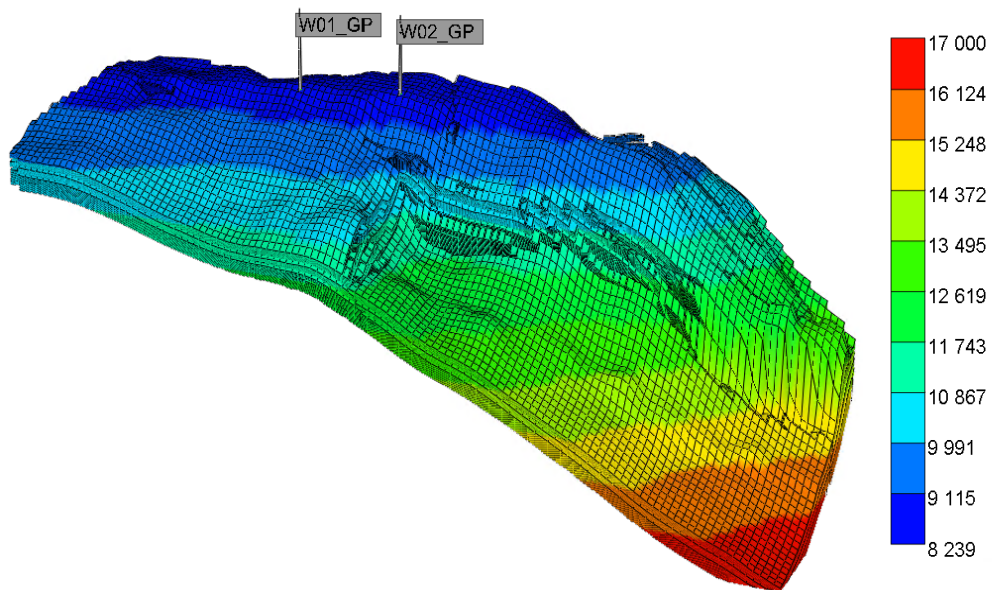


Figure 4-3: the 3D view of the grid top from CMG Builder

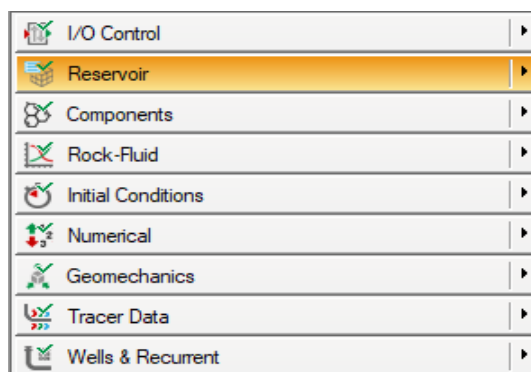


Figure 4-4: Model Tree from CMG Builder

Figure 4-4 shows the model tree in builder that is followed to define the model properties as in next sections

### 4.3 I/O Control

In this section, we define the simulation outputs. We made sure, in addition to the default outputs, to have added the mole fraction of different components.

### 4.4 Reservoir

In this section, the reservoir properties are defined. The grid and reservoir properties are directly taken from the RESCUE files exported from the original Eclipse model. Table 4-2 shows description of the properties used to define the reservoir section in our simulation model, as we see all the properties are directly imported as INCLUDE files from the original Eclipse model.

Table 4-2: Simulation model reservoir properties

Property	Value and Description
Component Global Composition	Defined as INCLUDE files for each component. The native fluids in the reservoir are mainly methane and water.
Permeability	Highly variable in all directions 0.1 ~ 100 mD Pore-volume-weighted average 93 mD in the horizontal direction and 59 mD in the vertical direction
Porosity	Defined as INCLUDE file Max value ~ 0.25 Average ~ 0.15
Pressure	Defined as INCLUDE file In the reservoir average value 500 psi
Water Saturation	Defined as INCLUDE file In the reservoir average value 0.1
Rock Compressibility	$9.814 \times 10^{-7}$ psi <sup>-1</sup>

## 4.5 Components

The fluid model was created in CMG-WinProp using the (Peng and Robinson 1976) equation of state. Table 4-3 shows the list of components used in the fluid model. The reservoir temperature is uniform and set at 183 °F.

Table 4-3: The list of components used to create a fluid model

Component	Pc (atm)	Tc (°K)
H2	12.80	33.2
CO2	72.90	304.7
N2	33.50	126.2
C1	45.44	190.6
C2	48.20	305.4
C3	41.90	369.8
C4	36.98	419.5
C5	33.15	465.9
C6	29.71	507.5
C7	29.00	548.0

## 4.6 Rock-Fluid

Figure 4-5 shows the relative permeability curve defined in the model. The gas saturation in the reservoir varies from 0.7 to 0.95. Therefore, the liquid phase can be considered an immobile phase in our model.

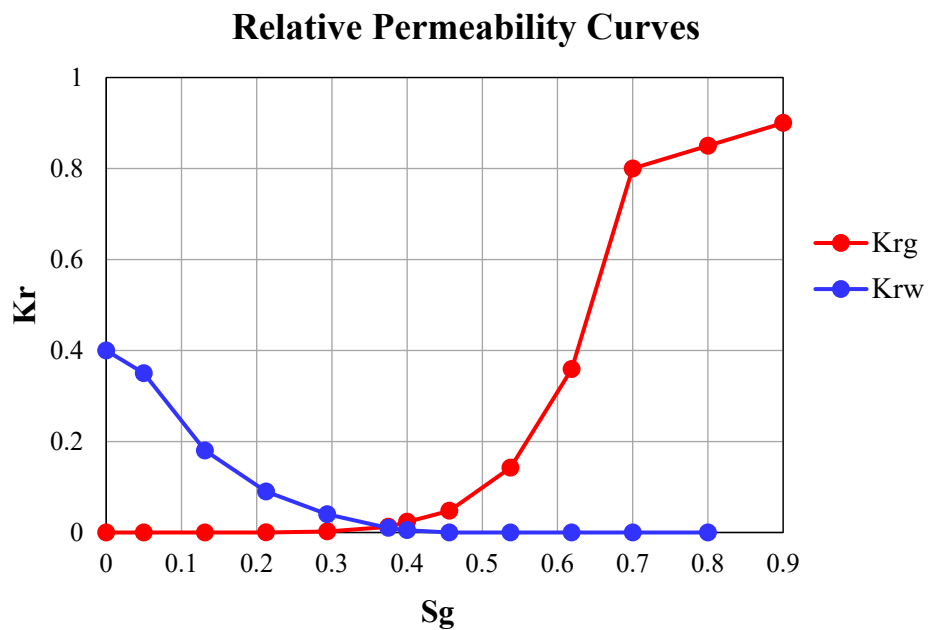


Figure 4-5: Relative permeability curves, red curve: gas, blue curve: water

## 4.7 Initial Conditions

The reservoir pressure, water saturation, and fluid composition are taken from the original Eclipse model, and the model is initialized by enumeration. Table 4-4 shows the average composition of the fluid.

*Table 4-4: Average initial composition*

Component	Mole Percentage
C1	90.3
C2	4.5
C3	1.2
N2	2.8
Others	1.2

## 4.8 Numerical

In this section we set the simulation running controls, such as timestep sizes and maximum changes. We left all default values except for normal saturation and composition change per timestep and set it to 0.1 instead of 0.15.

## 4.9 Well and Recurrent

In this section, the wells completions, perforation intervals, well events, well constraints, wellbore model, and injected fluid composition are defined.

As we are planning to cycle the hydrogen five times, so we first defined date range from 01-Jan-2031 till 01-Mar-2037, and to leave the first year for preparation of the storage either by fill-up or injecting cushion gas. Then, we defined two vertical wells, and each well is used as a producer well and an injector well. As Figure 4-3 shows, the two wells are located in the crest of the reservoir. Therefore, at the end we have two producers and two injectors named W01-GP, W01-GI, W02-GP, and W02-GI.

Then the well events and constraints are defined. As Figure 4-6 shows, the well events and the wells' periods on injection are shown in red (production is shown in black). As seen in the figure, hydrogen is injected during summer (March to September), when the electricity demand is low, followed by three months, then starts the production and retrieval of the stored hydrogen during winter (December to March). The first year is left for pressurizing the reservoir either with hydrogen or cushion gas.



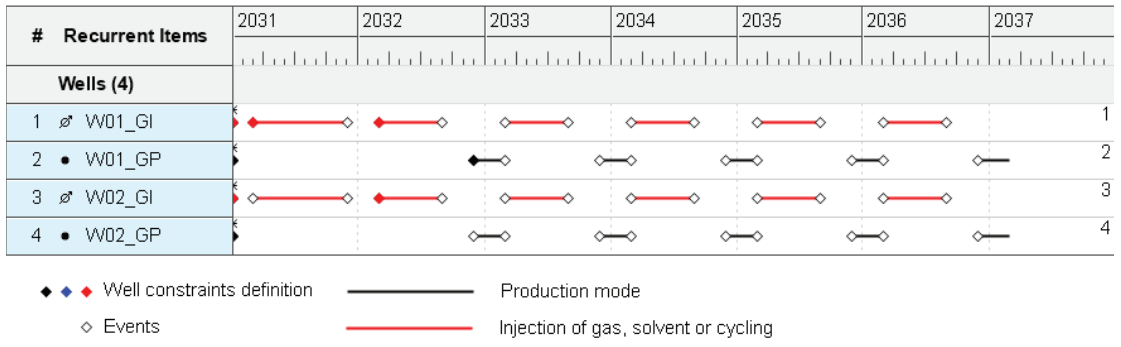


Figure 4-6: Timetable for injection and production



# Chapter 5

## Simulation of UHS in Viking A Field

Now we have a complete model of Viking A, and ready to start the dynamic simulation. In this chapter we will discuss the different dynamic behaviors of hydrogen in a larger real scale. Different scenarios will be run to show the effects of different factors.

### 5.1 Base Case

The base case consists of fill-up the reservoir with hydrogen for 9 months with injection rate of 30 MMscf/day/well. Then start cycling with the strategy shown in Table 5-1. These rates are concluded after trying different rates so that the reservoir is capable of producing at 40 MMscf/day/well for three months double the injection rate of 20 MMscf/day/well for 6 months.

*Table 5-1: Base Case strategy*

	Rate	Period
Fill-up	30 MMscf/day	9 months
Shut-in	--	3 months (September-November)
Production	40 MMscf/day	3 months (December-February)
Injection	20 MMscf/day	6 months (March-August)

Production starts in December till February during winter when consumption is expected to be the highest, then injection begins in summer and shut-in for three months.

For the wellbore models, and as we are injecting hydrogen and the native fluid in the reservoir is mainly methane, we decided here to run to sub-scenarios, using two lift tables because the composition of the produced gas is unknown.: (1) H2 lift table: assuming the produced gas is pure hydrogen. (2) C1 lift table: assuming the produced gas is pure methane.

The lift tables are built using the PIPESIM tool. This should be mentioned that (Gray 1978) correlation is used for vertical flow calculation. Table 5-2 shows the parameters used in PIPESIM model to generate the lift tables.

Table 5-2: The parameters used to define the well model in PIPESIM

	<b>Bottom MD (ft)</b>	<b>ID (in)</b>	<b>Wall Thickness (in)</b>	<b>Roughness</b>
<b>Casing 1</b>	9300	8.681	0.472	0.001
<b>Tubing</b>	8300	4.95	0.275	0.001

Table 5-3 shows the constraints defined for different periods for injectors and producers in different phases.

Table 5-3: The well constraints defined in the simulation model

<b>Phase</b>	<b>Parameter</b>	<b>Value</b>
<b>Filling-up</b>	Well-head pressure	800 (psi)
	Injection rate	30 (MMSCF/day/well)
<b>Hydrogen injection cycling</b>	Well-head pressure	800 (psi)
	Injection rate	20 (MMSCF/day/well)
<b>Production</b>	Well-head pressure	100 (psi)
	Production rate	40 (MMSCF/day/well)

### 5.1.1 Base case results

Figure 5-1 shows the gas production rates for the entire field, for well W01 from 2030 to 2037 end of the fifth cycle for the base case.

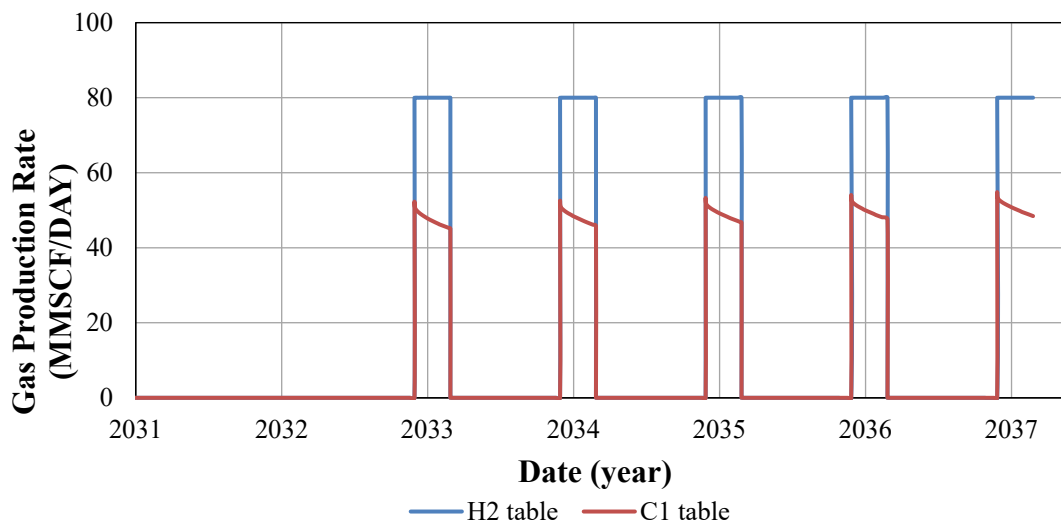


Figure 5-1: Total gas production profile of standalone GEM model using H2 lift table (Blue) vs. C1 lift table (Orange)

As can be seen in this figure, the field can produce at the target of 40 MMSCF/day/well (i.e., 80 MMSCF/day in total for two wells) when using a 100% hydrogen lift table. However, it cannot if a methane lift table is being used.

Figure 5-2 shows well-head and bottom-hole pressure for well W01 from 2031 to 2037, i.e., the end of the fifth cycle for the base case. As can be seen, the WHP constraint of 100 psi is violated, and consequently, a desirable production rate cannot be reached when using the C1 table.

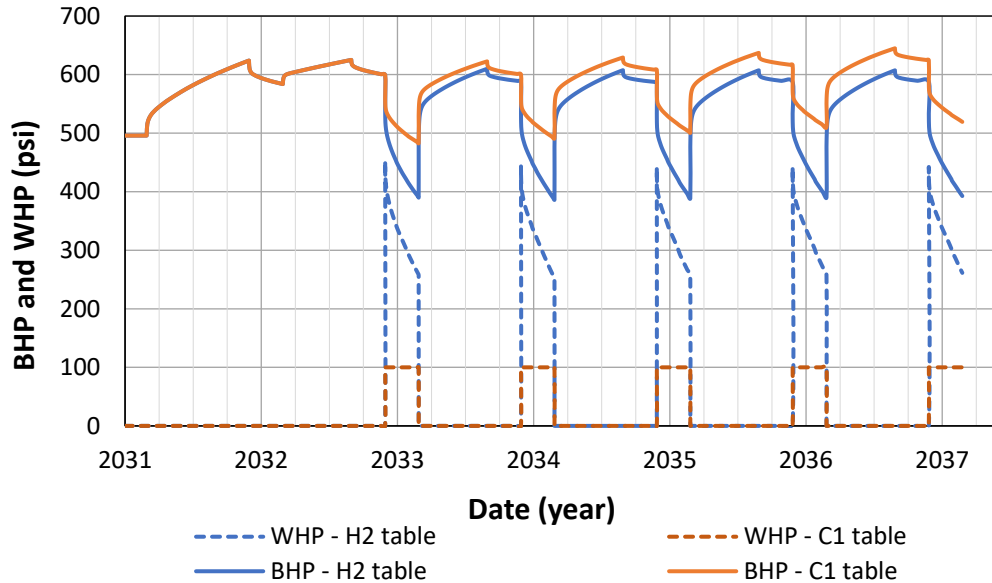


Figure 5-2: Well-head-pressure and bottom-hole pressure of well W01

This should be noted that the difference between BHP and WHP significantly impacts the rate and composition of the produced fluid. As can be seen at the beginning of the production cycle, hydrogen purity is high (the gas column is lighter); this implies that the pure hydrogen lift table can describe the production fluid (blue curves); however, as production continues, the impurities increases in the produced gas and more methane are being produced (the gas column is gradually getting heavier). Therefore, the production moves toward the orange curves (pure methane lift table).

Figure 5-3 shows the hydrogen mole fraction in the produced gas stream, which varies over time.

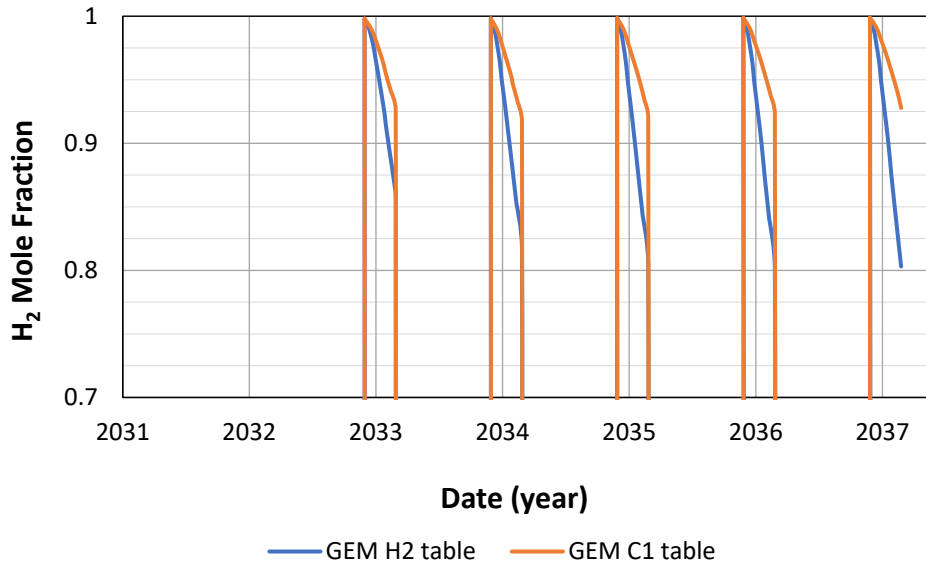


Figure 5-3: Mole fraction of hydrogen with different lift tables

As can be seen, the hydrogen percentage decreases for both cases as more native gas (methane) is produced over time. Moreover, the hydrogen percentage is lower when the H2 lift table is used.

It can be concluded from the above results that the lift table has a significant impact when using a standalone simulator. In practice, a mixture of gases (hydrogen, methane, small fraction of the other gases) is produced. In the beginning, the produced gas is pure hydrogen which then its composition gradually decreases over time while the composition of other gases increases. Utilizing individual lift tables alone (H2 or C1) cannot describe the production system accurately. This can only be modeled by an integrated coupled model, which captures compositional changes of the produced fluid over time (see next section).

## 5.2 Integrated Asset Model with CoFlow

Integrating the reservoir model with the well model will have more realistic results, because the lift tables are composition-dependent. This means neither 100% hydrogen nor 100% methane is produced and should be in between. This can be implemented using IAM.

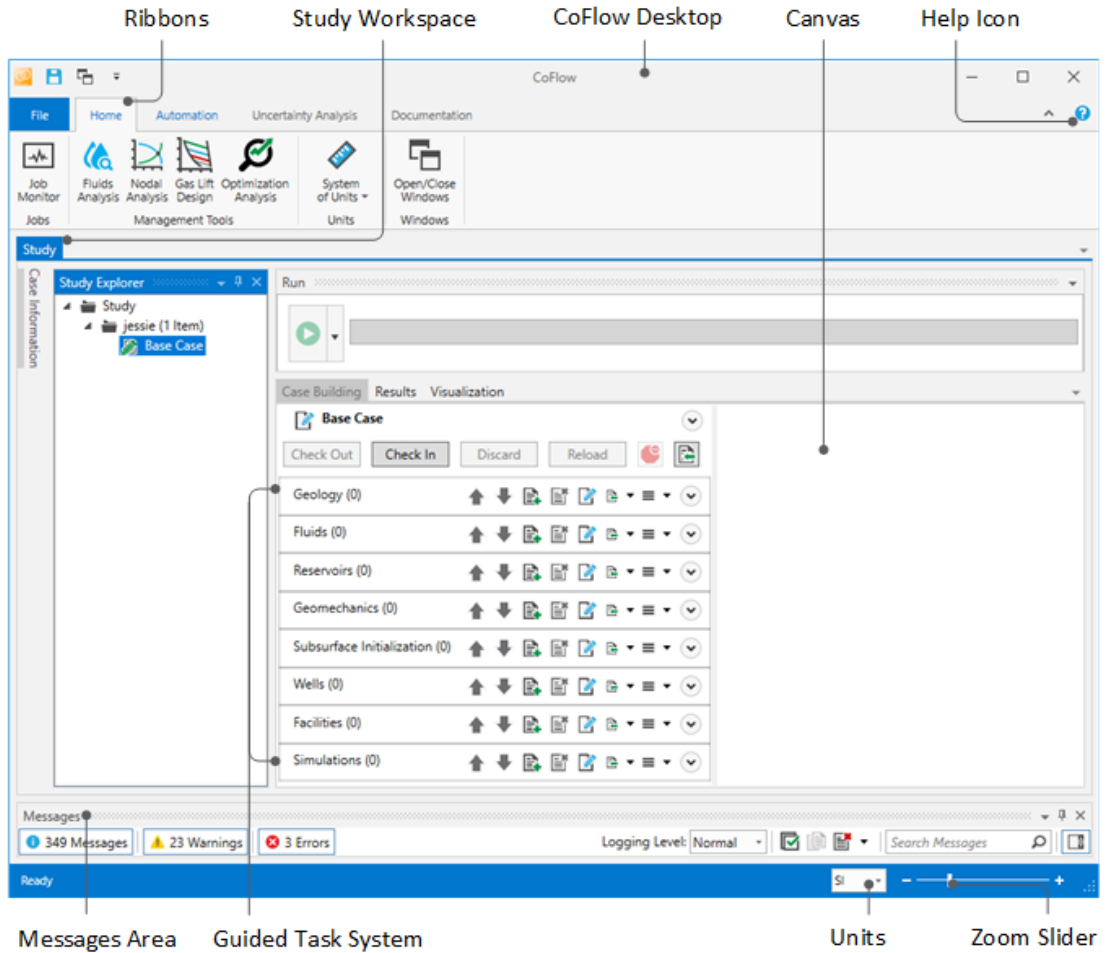


Figure 5-4: CoFlow interface for the Guided Task panel (Computer Modelling Group Ltd 2021)

## 5.2.1 CoFlow model setup

This section explains how the IAM model is built. Figure 5-4 shows the interface for the Guided Task panel with which we built our integrated model.

### 5.2.1.1 Reservoir and fluid model

The reservoir model is imported into CoFlow as a GEM dataset to use the same reservoir model established for GEM. Also, the same Fluid Model generated using WINPROP is used and imported to CoFlow.

### 5.2.1.2 Define the wells

To define the wells in the CoFlow model, first from the GEM model a RESCUE file is generated for the wells then imported in the CoFlow. In the next step, the perforations and equipment are defined as in the base case except for the well model, as the target from using IAM technology is to integrate between the standalone models, therefore, the well model is

defined in CoFlow using (Gray 1978) correlation for gas wells, and also, the heat transfer coefficient is defined to be 3 Btu/(ft<sup>2</sup>\*hr\*degFDif).

Figure 5-5 shows the Rate constraints that used for both wells (W01 & W02), for the producer the production limit is set to 40 MMSCF/DAY and the WHP to minimum 100 PSI. and the injector limits are set to 30 MMSCF/DAY for cushion gas period and 20 MMSCF/DAY for hydrogen cycling and the BHP to 2000 PSI.

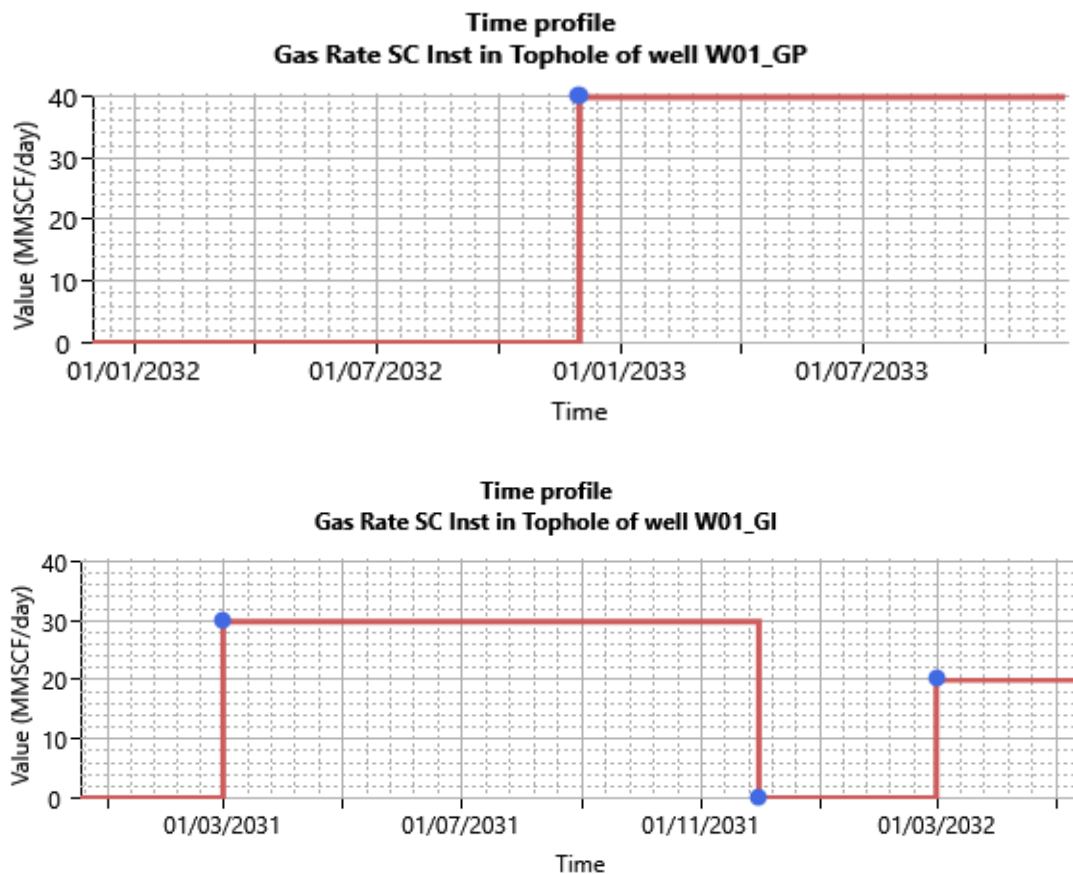


Figure 5-5: the Time profile constraints setup for W01\_GP & W01\_GI

In the next step, the well simulation time events are defined to be as the same strategy in the base case, refer to Table 5-1. As a last step in wells definition, we coupled between the wells created in CoFlow and wells defined in GEM dataset.

### 5.2.1.3 Creating Injection and Production Facility

Figure 5-6 shows the simple surface facility built to integrate the reservoir and well model. Each injector has two sources, one for cushion gas (de-activated in base case as we are filling-up with hydrogen) and one for cycling hydrogen, the properties of the sources are set to match the base case strategy (the shut-in and start times, flowrate limits, fluid type...etc). The two producers are connected to 2-phase separator.



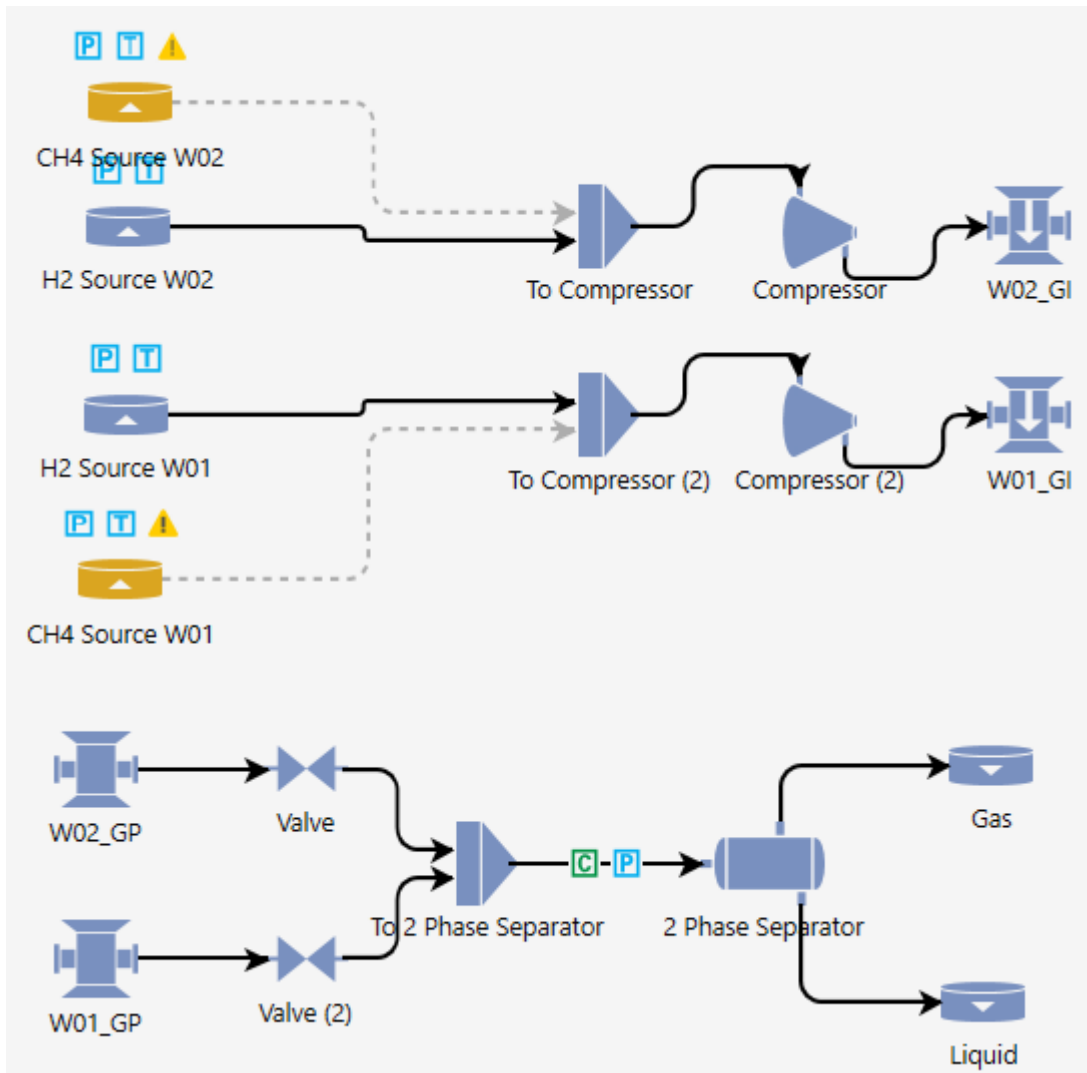


Figure 5-6: Surface facility schematic in CoFlow

### 5.2.2 CoFlow results

The CoFlow module is used to accurately couple the reservoir-wellbore production system. It was already demonstrated that a standalone model with a lift curve of either 100% methane or 100% hydrogen are unrealistic. Due to the nature of UHS, the producing gas changes over time, and using a lift table with a fixed composition leads to inaccurate results.

Figure 5-7 shows the results from CoFlow, which considers the compositional changes for pressure drop calculations in the wellbore against the results of the standalone model. In the flow model, the so-called shaking hand frequency is set daily basis; this means that the rate at which the GEM reservoir model will deliver (shake hand) its data (IPR, composition, and well indices) to the well model is evaluated daily, this will increase the simulation time considerably, but it gives more accurate results.

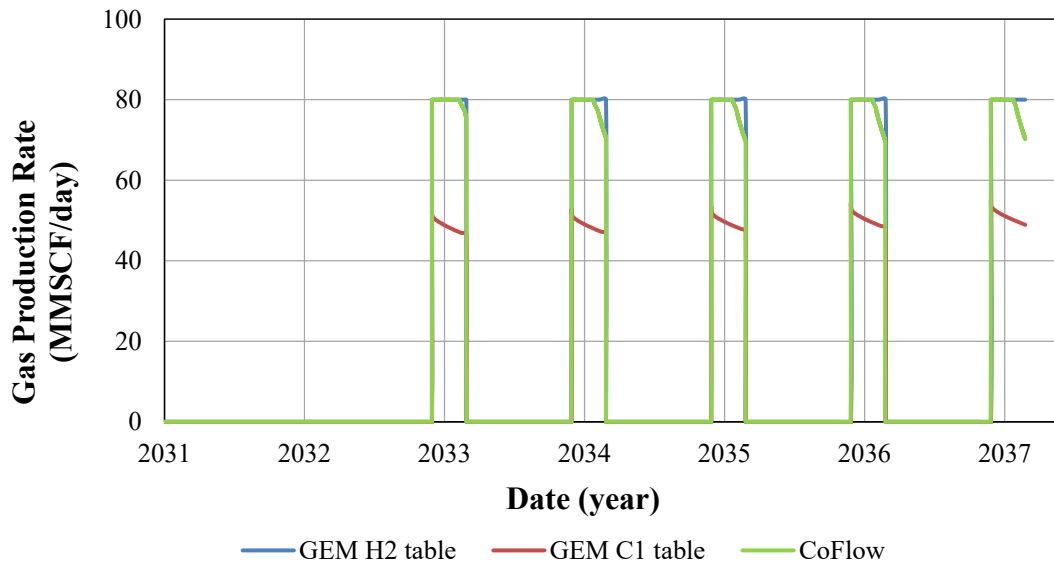


Figure 5-7: Total gas production rate GEM vs. CoFlow

From the CoFlow results above, it can be seen that the field cannot produce the aimed target of 40 MMscf/day/well (i.e., 80 MMSCF/day in total for two wells) for the three months, especially after the first cycle. This shows that the initial reservoir pressure is not high enough to support continuous production. Perhaps, a longer fill-up period and/or higher injection rate is required to achieve the target rate. This effect is much more pronounced in the hydrogen compositional plot shown in Figure 5-8 when the hydrogen mole fraction drops well below 90%, again showing that the reservoir pressure is not enough before cycling starts.

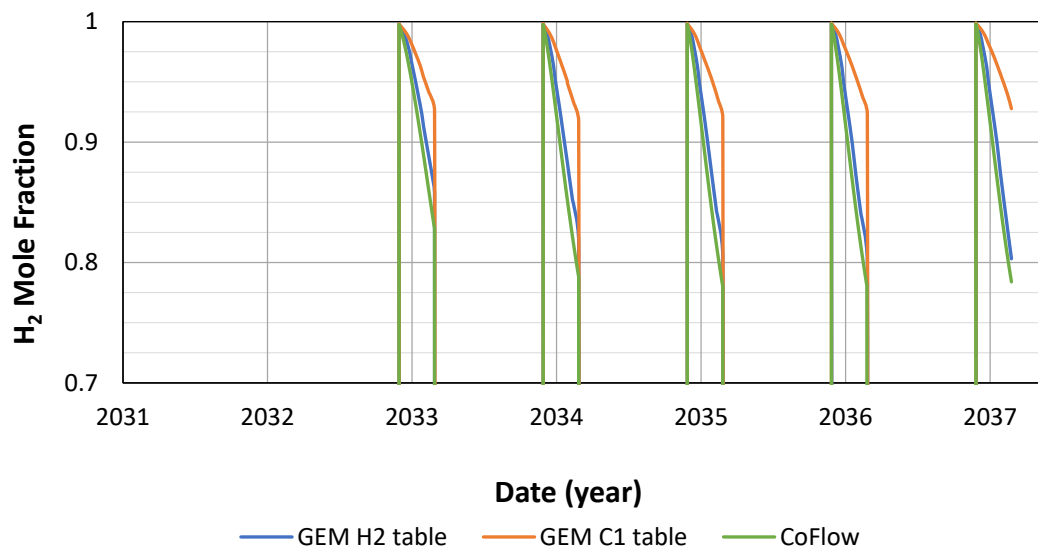


Figure 5-8: Hydrogen mole fraction in the produced stream

The above results show that coupling the reservoir and wellbore will improve the prediction of the whole production system.

# Chapter 6

## Sensitivity Analysis

### 6.1 Cushion gas type

For this analysis, the CoFlow module is used to investigate the impact of different cushion gases on the performance of the UHS in the Viking A field; it should be mentioned that all other properties are kept similar to the base case.

Figure 6-1 shows the gas production rates when using the different cushion gases. It can be concluded that the lighter the cushion gas, the more hydrogen can produce, especially at early cycles. However, the effect of the cushion gas on the production rate diminishes for later cycles.

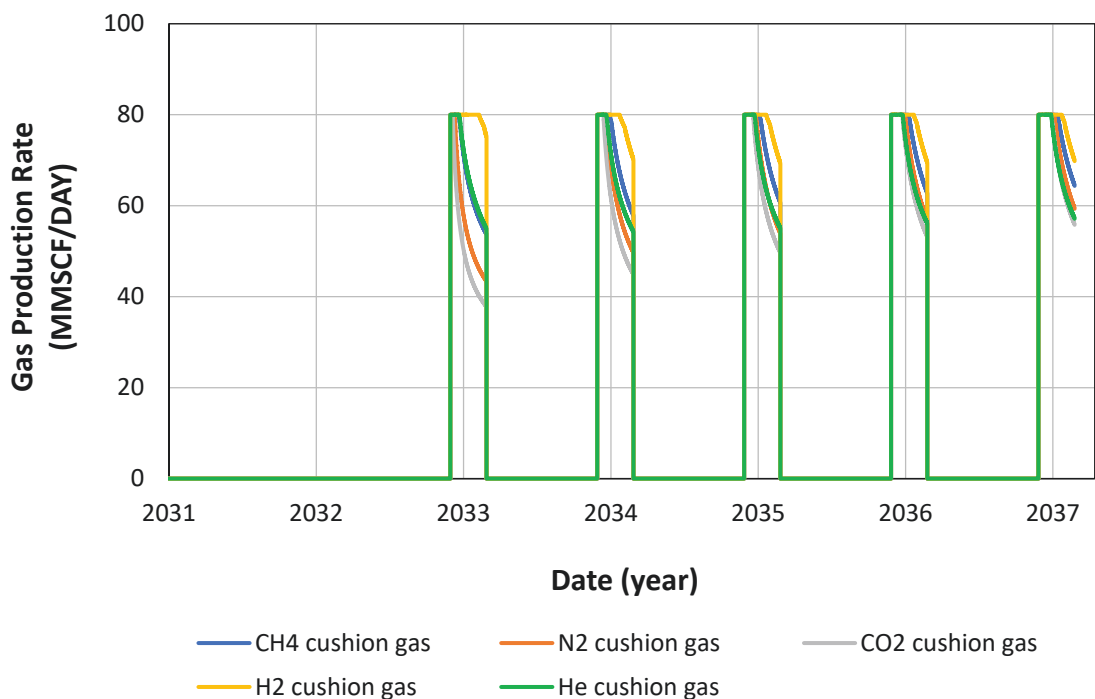


Figure 6-1: Gas production rate of the field for different cushion gases using CoFlow

Figure 6-2 shows the mole fraction of hydrogen in the produced fluid. When we fill up the reservoir with hydrogen before cycling, it gives higher purity of produced hydrogen. But again, this effect is more visible in early cycles and diminishes in later cycles, and in the fifth cycle, almost equal purity for all cases will be obtained.

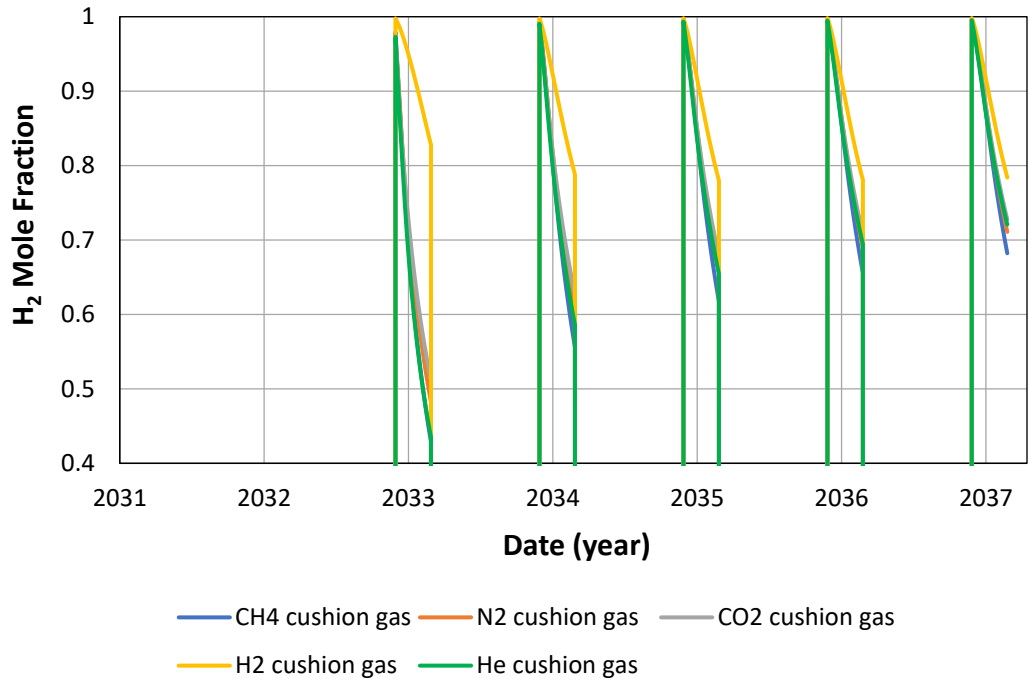


Figure 6-2: Mole fraction of produced hydrogen with different cushion gases using CoFlow

During these scenarios, 53.3 BSCF of gas in total has been injected, of which 16.5 BSCF during the cushion gas/fill-up injection period and 36.8 BSCF of cycling hydrogen. Figure 6-3 shows the amounts produced and remaining hydrogen with different cushion gases.

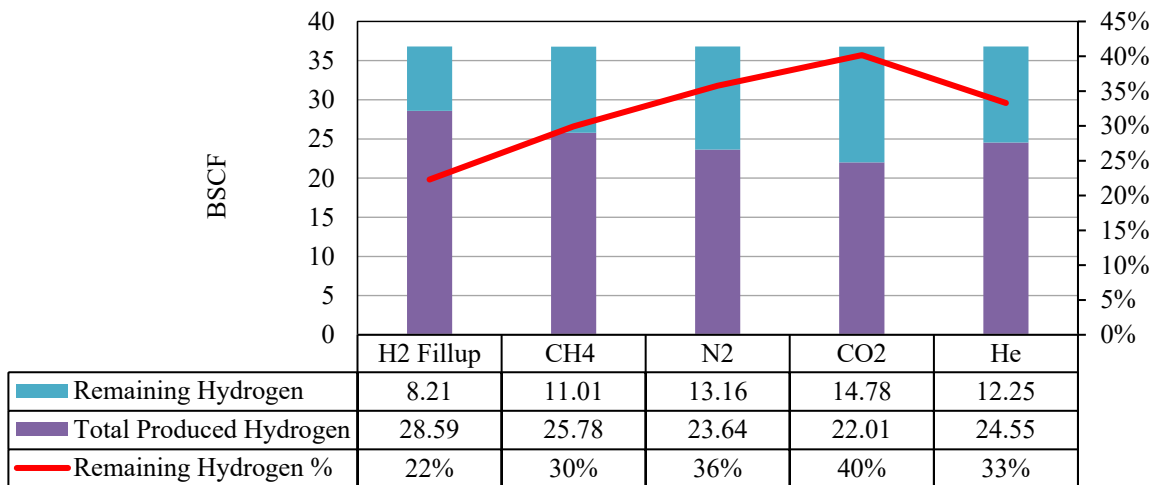


Figure 6-3: The total produced and remaining hydrogen after five cycles of hydrogen injection with different cushion gases

It is shown that when CO<sub>2</sub> is used as cushion gas, 40% of the injected hydrogen remains and cannot be produced back, which resembles the worst performance compared to other scenarios. This result shows that only 22% of the cycling hydrogen remains in the reservoir when the reservoir is filled-up with hydrogen before cycling starts.

Among other cushion gases, methane performs best, with 30% remaining hydrogen. However, an economic study should be conducted to evaluate the feasibility of such scenarios, as hydrogen is considerably more expensive than other gases. Furthermore, the cost of the separation processes at the surface should also be included in the feasibility study.

## 6.2 Diffusion effect

The hydrogen has very high diffusivity, about 0.61 cm<sup>2</sup>/s, almost four times more than methane. Therefore, hydrogen diffusion to the surroundings could affect the project's economy. As the CoFlow simulation with diffusion takes a much longer time, the effect of diffusivity is examined using a standalone GEM simulator with a pure hydrogen lift table. To add the effect of diffusion in the GEM model, the (Sigmund 1976) is utilized to calculate the binary diffusion coefficient between different components in the mixture and add the following line to the GEM code in the COMPONENT PROPERTIES section:

\*DIFCOR-GAS \*SIGMUND

Figure 6-4 and Figure 6-4 compare the purity of the produced hydrogen and methane with and without the diffusion effect.

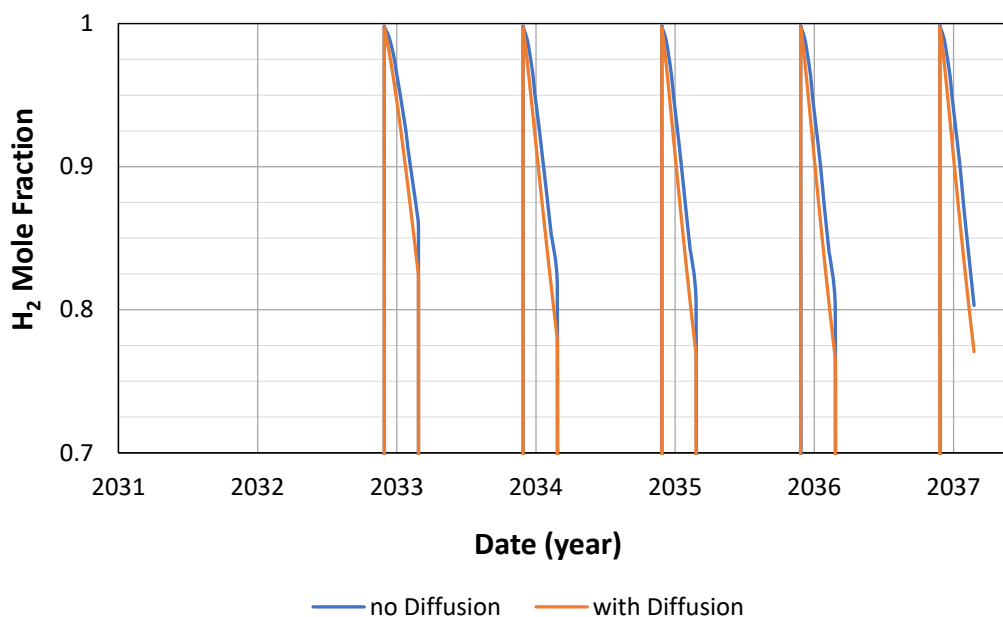


Figure 6-4: Mole fraction of hydrogen with and without diffusion

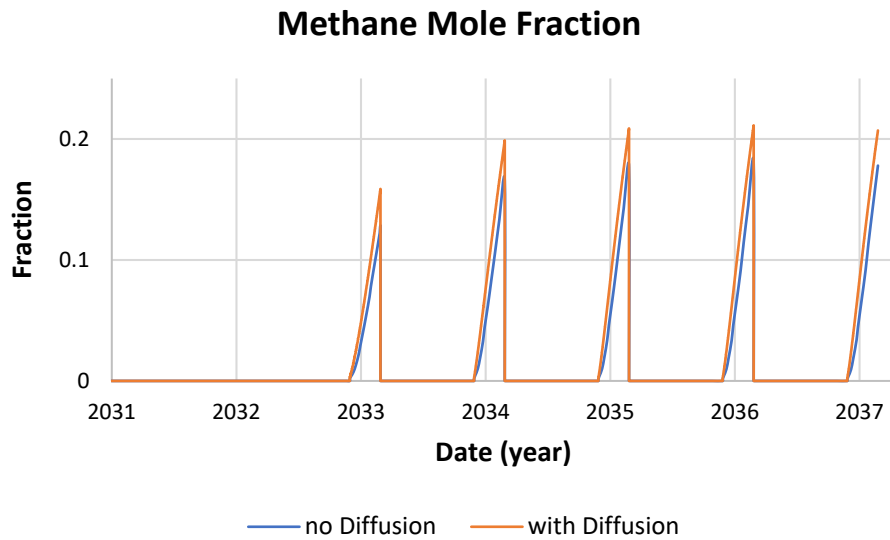


Figure 6-5: Mole fraction of methane with and without diffusion

As expected, hydrogen diffuses into the reservoir and is mixed up with the native fluids (mainly methane) to some extent, producing more methane. However, the impact of diffusion is marginal because diffusion is a prolonged process that would be more effective at the time scales beyond the injection/production intervals.

### 6.3 Extended/longer fill-up period

An important metric to evaluate the performance of the UHS is the purity of the produced hydrogen because this will affect the surface processing operations and, in turn, the operating expenses. To enhance the purity, the fill-up period is extended from 9 months to 2 years with the same rate of 30 MMSCF/day/well of hydrogen (i.e., 60 MMSCF/day in total for two wells), as shown in Figure 6-6.

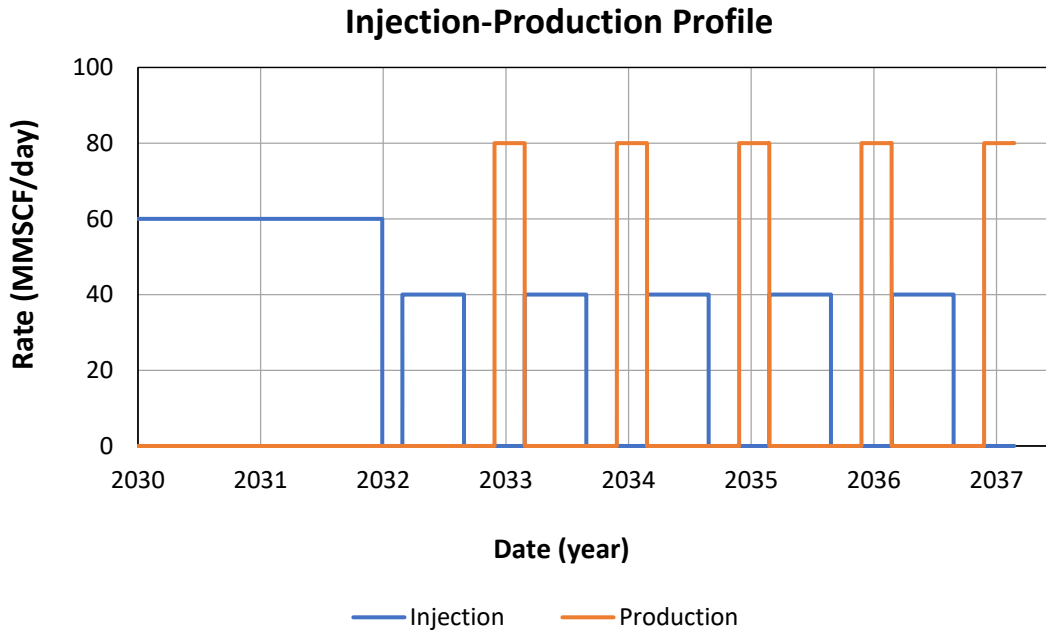


Figure 6-6: Injection-Production profile of the whole field with an extended fill-up period

After extending the fill-up period, the reservoir can maintain the target of 40 MMSCF/day/well (i.e., 80 MMSCF/day in total for two wells) for the three-month production period. This is due to the increased BHP compared to the 9-month fill-up period, as shown in Figure 6-7.

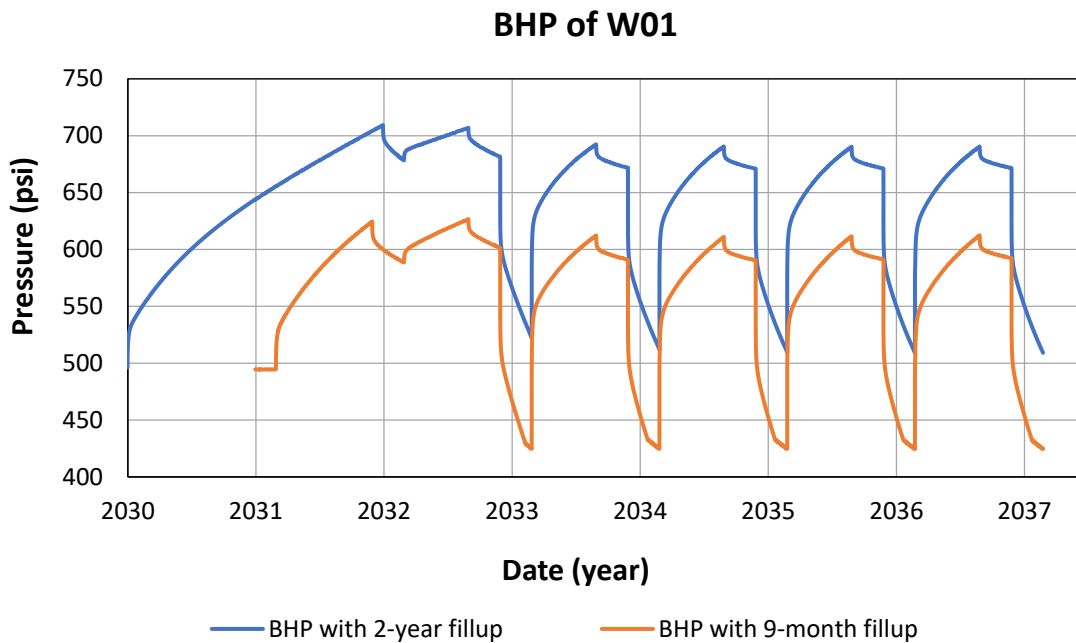


Figure 6-7: BHP of W01 with 2-year fill-up and 9-month fill-up

Figure 6-8 shows that the purity of produced hydrogen is enhanced to some extent, but a considerable amount of produced methane will still require surface processing.

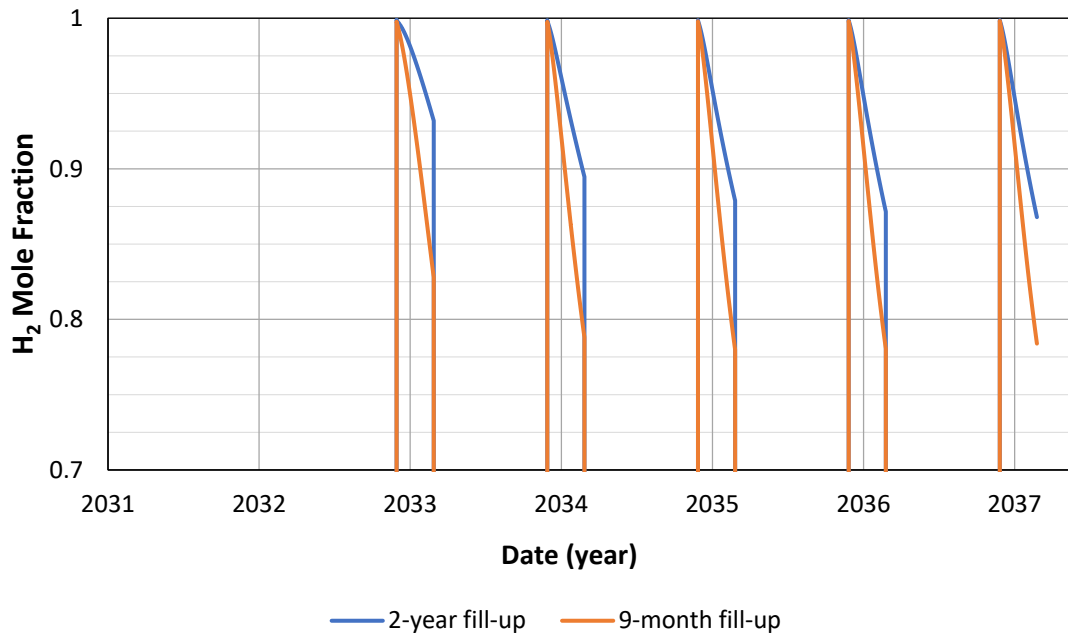


Figure 6-8: H<sub>2</sub> mole fraction with 2-year fill-up and 9-month fill-up

Figure 6-9 shows that, in the 2-year fill-up period, 43.8 BSCF hydrogen is injected vs. 16.5 BSCF in the 9-month fill-up case, and the produced hydrogen is increased only by 9%. This is because the hydrogen dissipates into the reservoir and does not remain in the well’s vicinity. Thus, the fill-up hydrogen doesn’t act as a good barrier, producing methane.

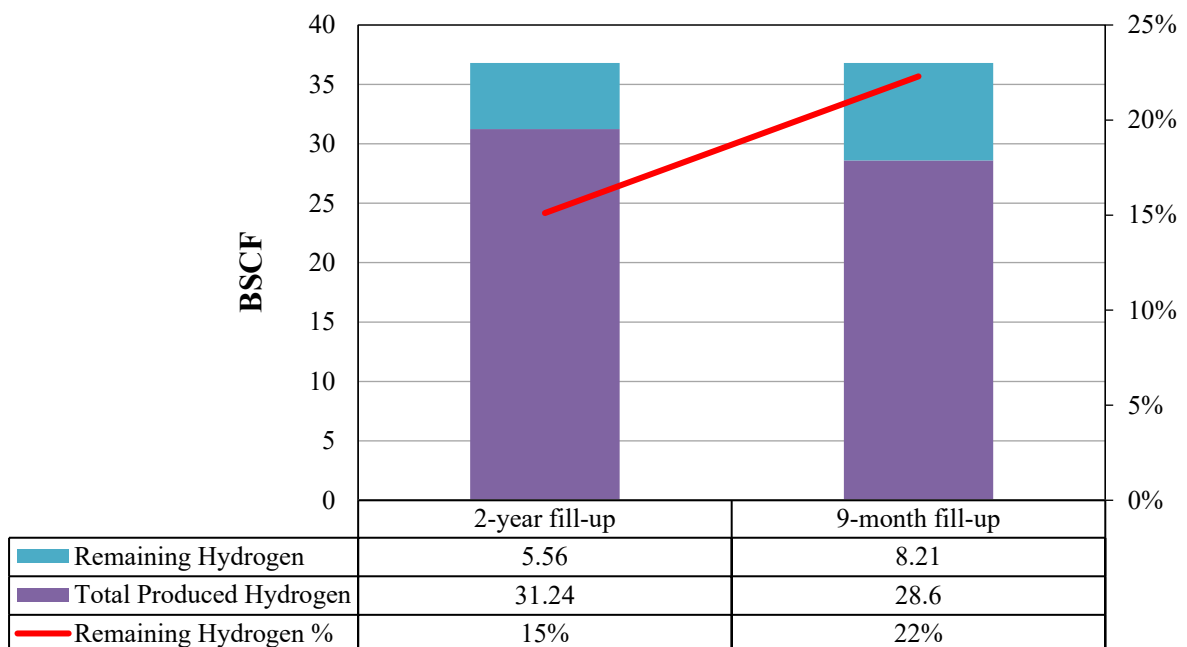


Figure 6-9: Produced and remaining hydrogen with 9-month and 2-year fill-up periods



## 6.4 Increased injection rate

It was shown in Figure 6-3 that among different cushion gases other than hydrogen, methane gives the best performance, with the lowest remaining hydrogen of only 30%. Methane, as a cushion gas, has an advantage over hydrogen due to its lower cost and availability. Thus, in this case, the hydrogen injection rate increases from 20 to 30 MMSCF/day/well.

Figure 6-10 shows that the target production rate is reached when the cycling injection rate increases, as more hydrogen is injected than produced.

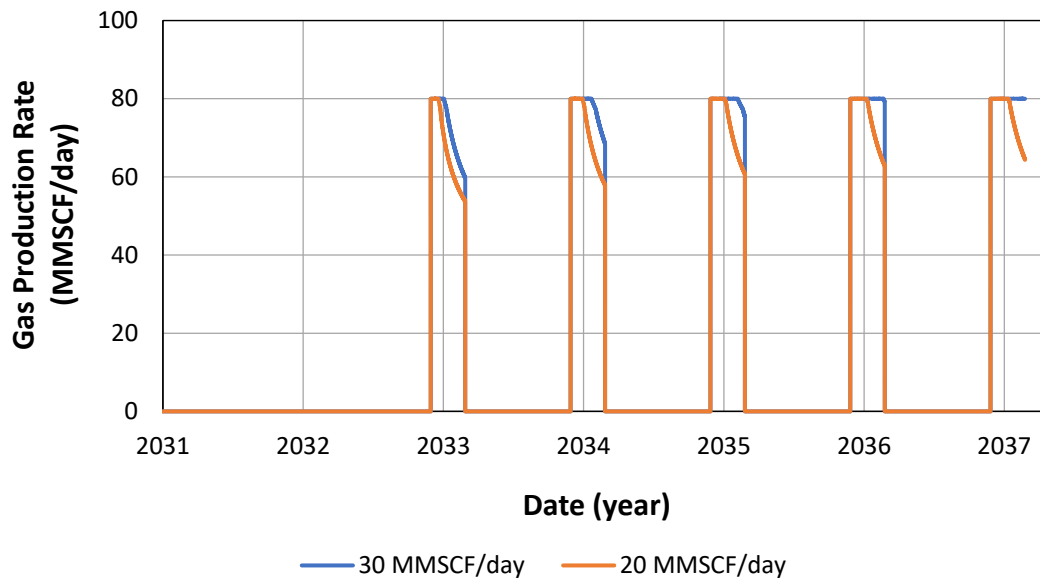


Figure 6-10: Gas production rate when using 20 and 30 MMSCF/day injection

Figure 6-11 shows that when the cycling injection rate increases, the purity of the produced hydrogen increases over time which is more desirable.

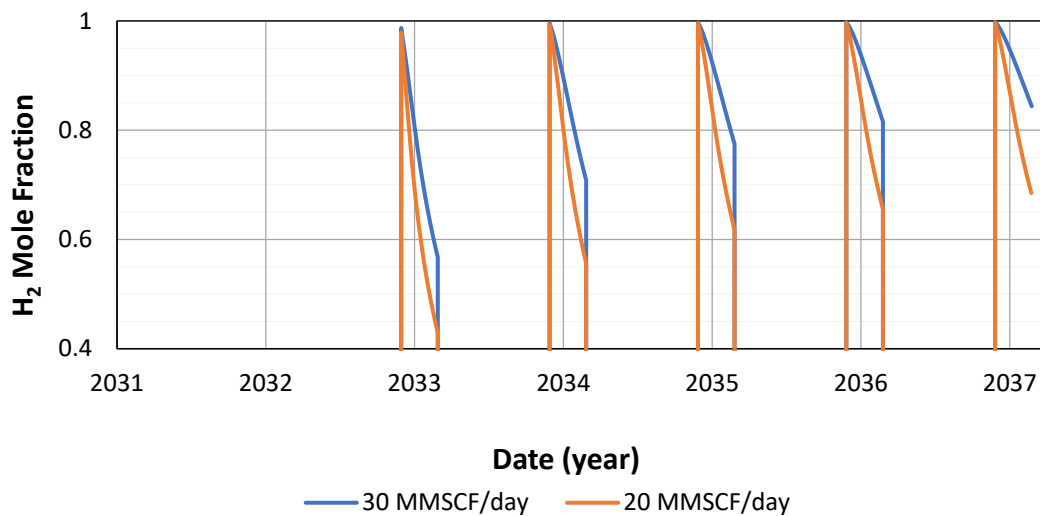


Figure 6-11: Mole fraction of produced hydrogen

Figure 6-12 shows that the efficiency is decreased considerably as 46% of the injected hydrogen remains in the reservoir compared to only 30% when injecting at a rate of 20 MMSCF/day.

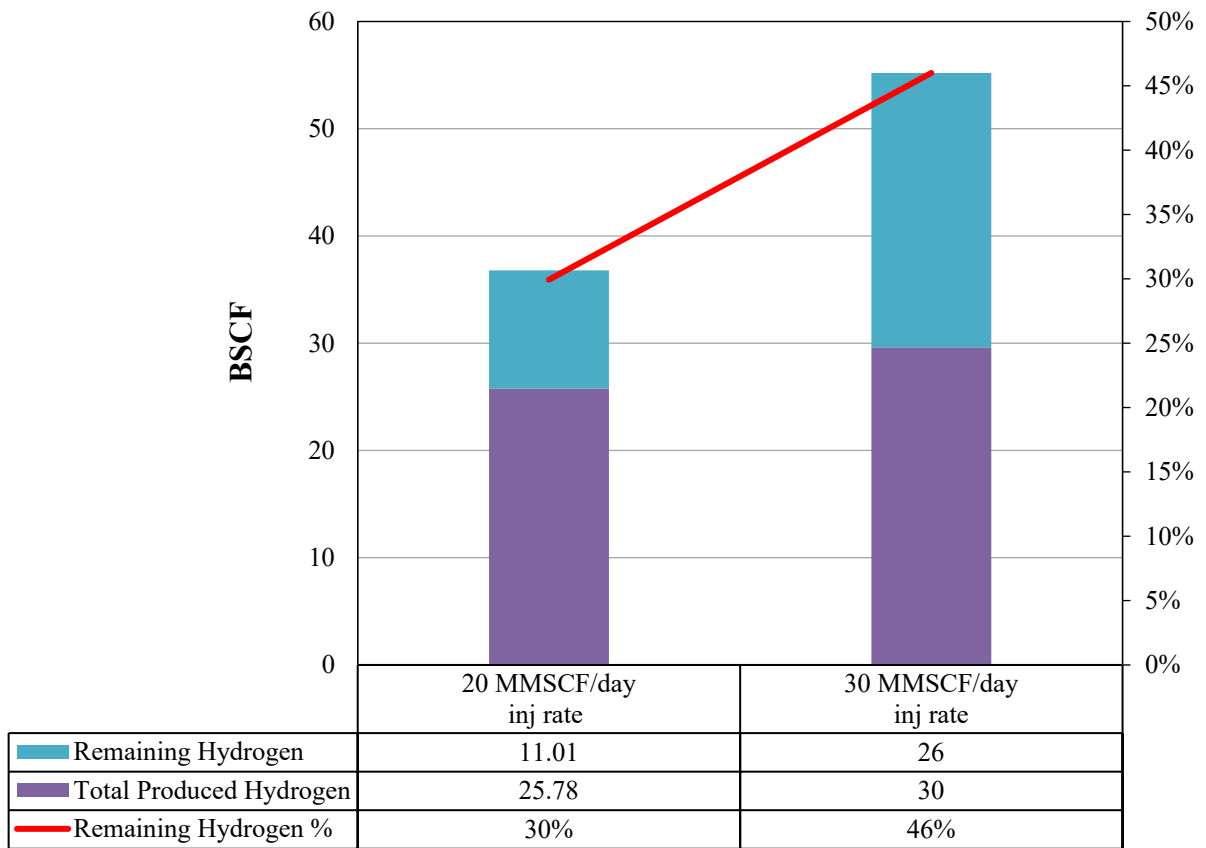


Figure 6-12: Produced and remaining hydrogen with 30 and 20 MMSCF/day cycling injection rate and methane as cushion gas

### 6.5 Shifted injection period

Instead of injecting hydrogen from March to September, the injection cycle is shifted to June-December as show in Table 6-1. Figure 6-13 shows that shifting the injection period decreased the remaining hydrogen by almost 1.2%.

Table 6-1: Injection-Production Strategy

Event	Period (month)	Rate (MMSCF/day)
Cushion gas (CH <sub>4</sub> )	9	30
Shut-in	3 (Mar-May)	--
Injection	3 (Jun-Nov)	20
Production	3 (Dec-Feb)	40

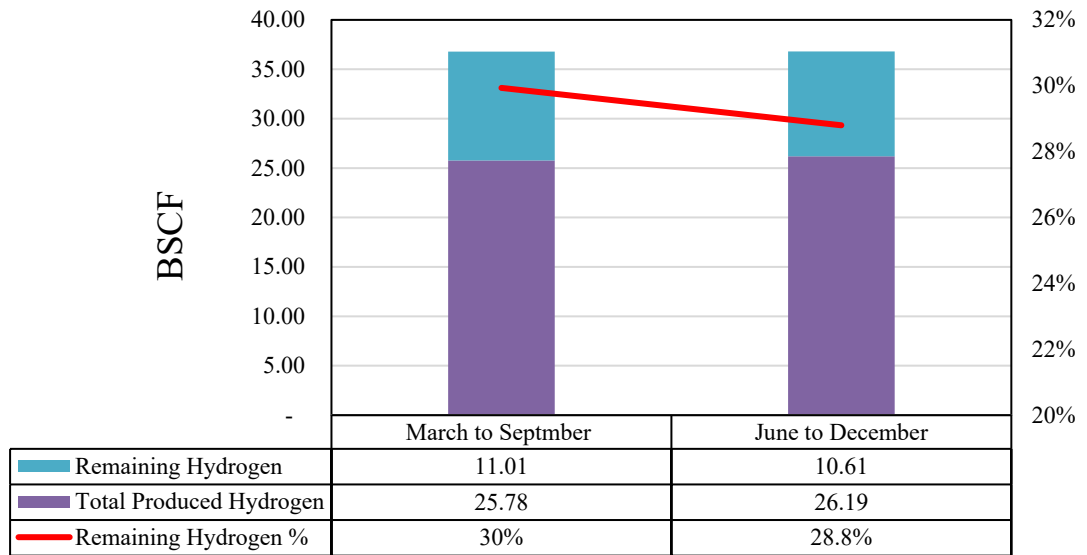


Figure 6-13: Produced, injected, and lost hydrogen with shifted injection cycle



# Chapter 7

## Conclusion

### 7.1 Summary

The objective of this dissertation is to demonstrate the technical viability and to show the role and importance of underground hydrogen storage technology in the inevitable energy transition from fossil fuels towards carbon-neutral fuels that the world is firmly following in compliance with the global agreements and initiatives that have been launched in the past few years, in an attempt to mitigate the global warming effects that harm our planet. following is a summary of the main points discussed in this study:

- The impacts of global warming have been explained and how the world is planning to tackle this threat.
- The efficiency of hydrogen as an energy carrier among other energy storage technologies is discussed in addition to the different methodologies of producing hydrogen
- Due to its unique physical and chemical properties, hydrogen behaves differently in porous media than natural gas, thus underground hydrogen storage encounters challenges and complexities. These challenges are addressed and discussed, in addition to the role of cushion gas as a pre-requisite to pressurize the reservoir and separate between the injected hydrogen and the existing fluids.
- Ongoing UHS projects are briefed to show the applicability and feasibility of this technology
- Conceptual model was built in a shape of “shoe box” using CMG to examine the behavior of the UHS under different conditions and the effects of different parameters on a small scale. Conclusions of this conceptual model study:

- Cushion gas type will affect the purity of the reproduced hydrogen, the rate, and the percentage of the reservoir native fluids in the produced stream. It was shown that the best cushion gas is the one that has density similar to the native existing fluids to avoid gravity override or underide.
  - Hydrogen diffusion can play a vital role in the feasibility of the UHS, as a considerable amount of hydrogen can be due to diffusivity.
  - Hydrogen has high bioactivity behavior and can be consumed in the subsurface due to this bioactivity. The methanogenesis process has been simulated and its effects in terms of hydrogen loss and reduced BHP is shown due to the interaction between CO<sub>2</sub> and H<sub>2</sub>.
  - The completion configurate is also studied, and it was concluded that the performance of the UHS can be enhanced when only operates the top part of the well and isolate the bottom that is exposed to the heavier existing fluids.
  - The geometry of the reservoir has an important effect, and it was shown that, the thinner reservoirs perform better for UHS, provided that it has a good upper and lower sealings.
- Viking A field in the North Sea was selected to continue the study on a real field.
  - To be able to capture the composition variation in the production stream and what effect it has on the vertical lift model, an integrated model was built using CoFlow, to integrate between the reservoir model and the well model. It was shown how powerful is the integrated model over the standalone reservoir model, in capturing the composition variation effect on the simulation results.
  - A sensitivity analysis was made to examine the different parameters' effect on the performance of the real field as a potential for UHS using the integrated model.

## 7.2 Future Work

Now we have a technical feasibility study for and UHS potential in the North Sea. And in order to complete this study, first a complete surface facility should be simulated, second an economic study should be carried out, to determine the most cost-efficient scenario and its net present value.

## References

- A., Pérez: E., Pérez: S., Dupraz: J., Bolcich: (Ed.) (2016): Patagonia Wind - Hydrogen Project: Underground Storage and Methanation. World Hydrogen Energy Conference. Spain, 13-16th June 2016. Spain. Available online at <http://www.whec2016.com/>.
- Acar, Canan; Dincer, Ibrahim (2020): The potential role of hydrogen as a sustainable transportation fuel to combat global warming. In *International Journal of Hydrogen Energy* 45 (5), pp. 3396–3406. DOI: 10.1016/j.ijhydene.2018.10.149.
- Amid, A.; Mignard, D.; Wilkinson, M. (2016): Seasonal storage of hydrogen in a depleted natural gas reservoir. In *International Journal of Hydrogen Energy* 41 (12), pp. 5549–5558. DOI: 10.1016/j.ijhydene.2016.02.036.
- AP, Reuters (2022): 4 EU countries pledge tenfold rise in North Sea wind power. In *Deutsche Welle*, 5/18/2022. Available online at <https://p.dw.com/p/4BTXq>.
- ARTHUR, T. J. (1993): Mesozoic structural evolution of the UK Southern North Sea: insights from analysis of fault systems. In *PGC* 4 (1), pp. 1269–1279. DOI: 10.1144/0041269.
- Baumgartner, L. K.; Reid, R. P.; Dupraz, C.; Decho, A. W.; Buckley, D. H.; Spear, J. R. et al. (2006): Sulfate reducing bacteria in microbial mats: Changing paradigms, new discoveries. In *Sedimentary Geology* 185 (3-4), pp. 131–145. DOI: 10.1016/j.sedgeo.2005.12.008.
- BAYKARA, S. (2004): Hydrogen production by direct solar thermal decomposition of water, possibilities for improvement of process efficiency. In *International Journal of Hydrogen Energy* 29 (14), pp. 1451–1458. DOI: 10.1016/j.ijhydene.2004.02.014.
- Carden, P.; Paterson, L. (1979): Physical, chemical and energy aspects of underground hydrogen storage. In *International Journal of Hydrogen Energy* 4 (6), pp. 559–569. DOI: 10.1016/0360-3199(79)90083-1.
- Computer Modelling Group Ltd (2021): CoFlow User Guide. Calgary: Computer Modelling Group Ltd. Available online at <https://www.cmgl.ca/>.
- Crotogino F; Hamelmann R (2007): Wasserstoff-Speicherung in Salzkavernen zur Glättung des Windstromangebots.
- European Commission. Directorate General for Energy. (2019): Clean energy for all Europeans: Publications Office.

- Foh, S.; Novil, M.; Rockar, E.; Randolph, P. (1979): Underground hydrogen storage. Final report. [Salt caverns, excavated caverns, aquifers and depleted fields].
- Gray, H.E (1978): Vertical flow correlation-gas wells.
- H.-O. Pörtner; D.C. Roberts; M. Tignor; E.S. Poloczanska; K. Mintenbeck; A. Alegría et al. (2022): Climate Change 2022: Impacts, Adaptation, and Vulnerability. Contribution of Working Group II to the Sixth Assessment Report of the Intergovernmental Panel on Climate Change. IPCC. Cambridge University Press. Available online at [https://www.ipcc.ch/report/ar6/wg2/downloads/report/IPCC\\_AR6\\_WGII\\_FinalDraft\\_FullReport.pdf](https://www.ipcc.ch/report/ar6/wg2/downloads/report/IPCC_AR6_WGII_FinalDraft_FullReport.pdf).
- Heinemann, N.; Booth, M. G.; Haszeldine, R. S.; Wilkinson, M.; Scafidi, J.; Edlmann, K. (2018): Hydrogen storage in porous geological formations – onshore play opportunities in the midland valley (Scotland, UK). In *International Journal of Hydrogen Energy* 43 (45), pp. 20861–20874. DOI: 10.1016/j.ijhydene.2018.09.149.
- HyStock (2019): The HyStock pilot project. Connecting Europe Facility. Netherlands. Available online at <https://www.hystock.nl/en>.
- IEA (2021): Global Hydrogen Review 2021. IEA. Paris. Available online at <https://www.iea.org/reports/global-hydrogen-review-2021>.
- IEA (2022): Monthly Electricity Statistics: Overview. IEA. Available online at <https://www.iea.org/reports/monthly-electricity-statistics-overview>.
- Kanaani, Mahdi; Sedae, Behnam; Asadian-Pakfar, Mojtaba (2022): Role of Cushion Gas on Underground Hydrogen Storage in Depleted Oil Reservoirs. In *Journal of Energy Storage* 45, p. 103783. DOI: 10.1016/j.est.2021.103783.
- Lemieux, Alexander; Sharp, Karen; Shkarupin, Alexi (2019): Preliminary assessment of underground hydrogen storage sites in Ontario, Canada. In *International Journal of Hydrogen Energy* 44 (29), pp. 15193–15204. DOI: 10.1016/j.ijhydene.2019.04.113.
- Licht, Stuart (2003): Solar Water Splitting To Generate Hydrogen Fuel: Photothermal Electrochemical Analysis. In *J. Phys. Chem. B* 107 (18), pp. 4253–4260. DOI: 10.1021/jp026964p.
- Moore, Jason; Shabani, Bahman (2016): A Critical Study of Stationary Energy Storage Policies in Australia in an International Context: The Role of Hydrogen and Battery Technologies. In *Energies* 9 (9), p. 674. DOI: 10.3390/en9090674.
- NSTA Authority (2022): UKCS Production. NSA Authority. UK. Available online at <https://www.nstauthority.co.uk/data-centre/nsta-open-data/production/>.
- Okoroafor, Esuru Rita; Saltzer, Sarah D.; Kovscek, Anthony R. (2022): Toward underground hydrogen storage in porous media: Reservoir engineering insights. In *International Journal of Hydrogen Energy* 47 (79), pp. 33781–33802. DOI: 10.1016/j.ijhydene.2022.07.239.
- Pale Blue Dot Energy (2017): Strategic UK CCS Storage Appraisal Project - Site 5: Viking. With assistance of UK Energy Research Centre Energy Data Centre (UKERC EDC), Pale Blue Dot, Axis Well Technology, Costain.



- Palmer, John R.; Tybero, Geir; Riches, Hugh A.; Dudley, Graham; Marsh, Marcus M. (1995): Renewed Exploration And Appraisal of the Viking Area: A Case Study. In : All Days. SPE Offshore Europe. Aberdeen, United Kingdom, 05-Sep-95 - 08-Sep-95: SPE.
- Panfilov, M. (2016): 4 - Underground and pipeline hydrogen storage. In Ram B. Gupta, Angelo Basile, T. Nejat Veziroğlu (Eds.): Compendium of Hydrogen Energy : Woodhead Publishing Series in Energy: Woodhead Publishing, pp. 91–115. Available online at <https://www.sciencedirect.com/science/article/pii/B9781782423621000043>.
- Peng, Ding-Yu; Robinson, Donald B. (1976): A New Two-Constant Equation of State. In *Ind. Eng. Chem. Fund.* 15 (1), pp. 59–64. DOI: 10.1021/i160057a011.
- Pfeiffer, Wolf Tilmann; Bauer, Sebastian (2015): Subsurface Porous Media Hydrogen Storage – Scenario Development and Simulation. In *Energy Procedia* 76, pp. 565–572. DOI: 10.1016/j.egypro.2015.07.872.
- Pudlo, Dieter; Ganzer, Leonhard; Henkel, Steven; Kühn, Michael; Liebscher, Axel; Lucia, Marco de et al. (2013): The H2STORE Project: Hydrogen Underground Storage – A Feasible Way in Storing Electrical Power in Geological Media? In Michael Z. Hou, Heping Xie, Patrick Were (Eds.): Clean Energy Systems in the Subsurface: Production. Berlin: Springer-Verlag Berlin and Heidelberg GmbH & Co. KG (Springer Series in Geomechanics and Geoengineering), pp. 395–412.
- RAG Austria AG; AXIOM angewandte Prozesstechnik GesmbH; VERBUND AG; MONTANUNIVERSITÄT LEOBEN; UNIVERSITÄT für Bodenkultur Wien; ENERGIEINSTITUT an der Johannes Kepler Universität Linz (2017): UNDERGROUND SUN STORAGE. Chemical storage of renewable energy in porous subsurface reservoirs with exemplary testbed. Vienna, Austria. Available online at <https://www.underground-sun-storage.at/en/public-relations/-/publications/publications-1.html>, checked on 7/21/2022.
- Riches, Hugh (2003): The Viking Field, Blocks 49/12a, 49/16, 49/17, UK North Sea. In *Memoirs* 20 (1), pp. 871–880. DOI: 10.1144/GSL.MEM.2003.021.01.73.
- Robert J. Hooper; Colin More (1995): Evaluation of Some Salt-Related Overburden Structures in the U.K. Southern North Sea. In M.P.A. Jackson, D. G. Roberts, S. Snelson (Eds.): Salt Tectonics: American Association of Petroleum Geologists, pp. 251–259.
- Schaber, Christopher; Mazza, Patrick; Hammerschlag, Roel (2004): Utility-Scale Storage of Renewable Energy. In *The Electricity Journal* 17 (6), pp. 21–29. DOI: 10.1016/j.tej.2004.05.005.
- Shi, Zhuofan; Jessen, Kristian; Tsotsis, Theodore T. (2020): Impacts of the subsurface storage of natural gas and hydrogen mixtures. In *International Journal of Hydrogen Energy* 45 (15), pp. 8757–8773. DOI: 10.1016/j.ijhydene.2020.01.044.
- Sigmund, Phillip M. (1976): Prediction of Molecular Diffusion At Reservoir Conditions. Part 1- Measurement And Prediction of Binary Dense Gas Diffusion Coefficients. In *Journal of Canadian Petroleum Technology* 15 (02). DOI: 10.2118/76-02-05.
- Stefano Patruno; William Reid (2016): Chronostratigraphic and structural framework for the Northern North Sea, Central North Sea and West of Shetlands (UKCS and NCS) (part of the PESGB "Structural Framework of the North Sea and Atlantic Margin" - 2017 Edition).

- Stolten, Detlef (Ed.) (2010): Proceedings / 18th World Hydrogen Energy Conference 2010 - WHEC 2010. Proceedings. World Hydrogen Energy Conference (18, 2010, Essen). Jülich: Forschungszentrum Jülich, Zentralbibliothek (Schriften des Forschungszentrums Jülich : Reihe Energie & Umwelt, vol. 78,4). Available online at <http://hdl.handle.net/2128/4325>.
- Tarkowski, Radosław; Czapowski, Grzegorz (2018): Salt domes in Poland – Potential sites for hydrogen storage in caverns. In *International Journal of Hydrogen Energy* 43 (46), pp. 21414–21427. DOI: 10.1016/j.ijhydene.2018.09.212.
- Taylor, J.; Alderson, J.; Kalyanam, K.; LYLE, A.; Phillips, L. (1986): Technical and economic assessment of methods for the storage of large quantities of hydrogen. In *International Journal of Hydrogen Energy* 11 (1), pp. 5–22. DOI: 10.1016/0360-3199(86)90104-7.
- Tek, M. R. (Ed.) (2013): Underground storage of natural gas. Theory and practice. Softcover reprint of the original 1st ed. 1989. Dordrecht: Kluwer Academic Publishers (NATO ASI series. Series E, Applied sciences, vol. 171).
- United Nations Framework Convention on Climate Change (2016): The Paris Agreement. FCCC/CP/2015/10/Add.1, revised 2018. Source: Paris Climate Change Conference. Available online at <https://unfccc.int/documents/184656>.
- van Hoorn, B. (1987): Structural evolution, timing and tectonic style of the Sole Pit inversion. In *Tectonophysics* 137 (1-4), pp. 239–284. DOI: 10.1016/0040-1951(87)90322-2.
- Veziroğlu, T. Nejat (1976): First World Hydrogen Energy conference, 1-3 March, 1976, Miami Beach, Florida. Conference proceedings, presented by International Association for Hydrogen Energy, [and] Clean Energy Research Institute, University of Miami ... / edited by T.Nejat Veziroğlu. Coral Gables, Florida: University of Miami.
- Wang, G.; Pickup, G.; Sorbie, K.; Mackay, E. (2021): Scaling analysis of hydrogen flow with carbon dioxide cushion gas in subsurface heterogeneous porous media. In *International Journal of Hydrogen Energy*. DOI: 10.1016/j.ijhydene.2021.10.224.
- Wang, Z.; Roberts, R. R.; Naterer, G. F.; Gabriel, K. S. (2012): Comparison of thermochemical, electrolytic, photoelectrolytic and photochemical solar-to-hydrogen production technologies. In *International Journal of Hydrogen Energy* 37 (21), pp. 16287–16301. DOI: 10.1016/j.ijhydene.2012.03.057.
- Ziegler, P. A. (1977): Geology and hydrocarbon provinces of the North Sea. In *GeoJournal* 1 (1). DOI: 10.1007/BF00189601.
- Zivar, Davood; Kumar, Sunil; Foroozesh, Jalal (2021): Underground hydrogen storage: A comprehensive review. In *International Journal of Hydrogen Energy* 46 (45), pp. 23436–23462. DOI: 10.1016/j.ijhydene.2020.08.138.

# List of Figures

Figure 1-1: Observed global and regional impacts due to climate change on the ecosystems and human systems (H.-O. Pörtner et al. 2022).....	12
Figure 1-2: Electricity Net Production and Consumption of Austria in 2021 (IEA 2022).....	13
Figure 1-3: Storage capacity for different energy storage technologies (Moore and Shabani 2016).....	13
Figure 1-4: Sources of Hydrogen Production (IEA 2021).....	14
Figure 1-5: Preferential areas of large-scale storage options (Stolten 2010).....	16
Figure 2-1: Mass and volume calorific values for different fuels at 200 bar and 25 °C (Crotagino F and Hamelmann R 2007).....	19
Figure 3-1: 3D view of the conceptual model.....	25
Figure 3-2: Production-Injection profile for the base case of the conceptual model.....	26
Figure 3-3: BHP during injection and production.....	27
Figure 3-4: Mole fraction of the produced gas.....	27
Figure 3-5: Hydrogen mole fraction in the produced gas.....	28
Figure 3-6: Mole fraction of methane in the produced gas.....	28
Figure 3-7: Different cushion gases mole fraction at the end of the first cycle.....	29
Figure 3-8: hydrogen mole fraction in the produced stream.....	30
Figure 3-9: Hydrogen mole fraction in the reservoir with and without diffusion after the end of first injection.....	30
Figure 3-10: Mole fraction of hydrogen with and without methanation.....	31
Figure 3-11: Bottom hole pressure with and without methanation.....	32
Figure 3-12: Hydrogen mole fraction when isolate the bottom part and only open the top third of the well.....	32
Figure 3-13: Mole fraction of hydrogen in case of thin reservoir against base case.....	33
Figure 4-1: Viking Field location map (Riches 2003).....	36
Figure 4-2: Production Profile of Viking A field (NSTA Authority 2022).....	36
Figure 4-3: the 3D view of the grid top from CMG Builder.....	37
Figure 4-4: Model Tree from CMG Builder.....	38
Figure 4-5: Relative permeability curves, red curve: gas, blue curve: water.....	39
Figure 4-6: the location of the two well trajectories.....	<b>Error! Bookmark not defined.</b>
Figure 4-7: Timetable for injection and production.....	41
Figure 5-1: Total gas production profile of standalone GEM model using H2 lift table (Blue) vs. C1 lift table (Orange).....	44
Figure 5-2: Well-head-pressure and bottom-hole pressure of well W01.....	45
Figure 5-3: Mole fraction of hydrogen with different lift tables.....	46
Figure 5-4: CoFlow interface for the Guided Task panel (Computer Modelling Group Ltd 2021).....	47
Figure 5-5: the Time profile constraints setup for W01_GP & W01_GI.....	48
Figure 5-6: Surface facility schematic in CoFlow.....	49
Figure 5-7: Total gas production rate GEM vs. CoFlow.....	50
Figure 5-8: Hydrogen mole fraction in the produced stream.....	50
Figure 6-1: Gas production rate of the field for different cushion gases using CoFlow.....	51
Figure 6-2: Mole fraction of produced hydrogen with different cushion gases using CoFlow.....	52
Figure 6-3: The total produced and remaining hydrogen after five cycles of hydrogen injection with different cushion gases.....	52
Figure 6-4: Mole fraction of hydrogen with and without diffusion.....	53
Figure 6-5: Mole fraction of methane with and without diffusion.....	54
Figure 6-6: Injection-Production profile of the whole field with an extended fill-up period ..	55
Figure 6-7: BHP of W01 with 2-year fill-up and 9-month fill-up.....	55
Figure 6-8: H <sub>2</sub> mole fraction with 2-year fill-up and 9-month fill-up.....	56

Figure 6-9: Produced and remaining hydrogen with 9-month and 2-year fill-up periods ..... 56  
Figure 6-10: Gas production rate when using 20 and 30 MMSCF/day injection ..... 57  
Figure 6-11: Mole fraction of produced hydrogen..... 57  
Figure 6-12: Produced and remaining hydrogen with 30 and 20 MMSCF/day cycling injection  
rate and methane as cushion gas ..... 58  
Figure 6-13: Produced, injected, and lost hydrogen with shifted injection cycle ..... 59

## List of Tables

Table 1-1: Comparison of the characteristic features of hydrogen and methane (Acar and Dincer 2020) .....	15
Table 3-1: Base case strategy for the conceptual model .....	26
Table 4-1: Viking gas fields data summary (Riches 2003).....	37
Table 4-2: Simulation model reservoir properties .....	38
Table 4-3: The list of components used to create a fluid model .....	39
Table 4-4: Average initial composition .....	40
Table 5-1: Base Case strategy .....	43
Table 5-2: The parameters used to define the well model in PIPESIM.....	44
Table 5-3: The well constraints defined in the simulation model.....	44
Table 6-1: Injection-Production Strategy.....	58



# Abbreviations

UHS	Underground Hydrogen Storage
IAM	Integrated Asset Modelling
SMR	Steam Methane Reformation
CAES	Compressed Air Energy Storage System
NG	Natural Gas
CCS	Carbon Capture and Sequestration
WHP	Well Head Pressure
BHP	Bottomhole Pressure
IPR	Inflow Performance Relationship
VLP	Vertical Lift Performance